Biosensors and Bioelectronics 141 (2019) 111451

Contents lists available at ScienceDirect

Biosensors and Bioelectronics

journal homepage: www.elsevier.com/locate/bios

Nucleic acids biosensors based on metal-organic framework (MOF): Paving the way to clinical laboratory diagnosis

Diaa I. Osman[a,b], Said M. El-Sheikh[c], Sheta M. Sheta[d,*], Omnia I. Ali[b], Aliaa M. Salem[c], Wafaa Gh Shousha[b], Sherif F. EL-Khamisy[e,f], Sherif M. Shawky[e,g,**]

[a] Clinical Biochemistry Department, National Liver Institute, Menoufia University, Menoufia, 32511, Egypt
[b] Chemistry Department, Faculty of Science, Helwan University, Cairo, 11795, Egypt
[c] Nanomaterials and Nanotechnology Department, Central Metallurgical R & D Institute, Cairo, 11421, Egypt
[d] Inorganic Chemistry Department, National Research Centre, 33 El-Behouth St., Dokki, Giza, 12622, Egypt
[e] Center of Genomics, Helmy Institute, Zewail City of Science and Technology, October Gardens, 6th of October City, 12578, Giza, Egypt
[f] Krebs Institute, Department of Molecular Biology and Biotechnology, University of Sheffield, Sheffield, S10 2TN, UK
[g] Biochemistry Department, Faculty of Pharmacy, Misr University for Science and Technology, 6th October City, Giza, 77, Egypt

ARTICLE INFO

Keywords:
Nucleic acids
Metal-organic frameworks
Biosensors
MOFs synthesis
Clinical applications

ABSTRACT

Development of ultra-sensitive, high specific and cost-effective nucleic acids (NAs) biosensors is critical for early diagnosis of cancer, genetic diseases and follows up response to treatment. Metal-organic frameworks (MOFs) as sensing materials underwent significant development in recent years due to their unique merits, such as structural diversity, tunable pore scale, large surface area, remarkable adsorption affinities, and good thermal stability. MOFs have shown potential contribution in nucleic acids biosensors research. Herein, a comprehensive overview on NAs biosensors state of the art based on MOFs has been discussed extensively, including different MOFs platforms sensing strategies (fluorescence, electrochemistry, electrochemiluminescence, and colorimetric techniques), their analytical performance and figures of merit in clinical diagnostics, with the future perspective in introducing MOFs in clinical laboratory diagnostics. Moreover, the different MOFs synthesis methods have been highlighted to serve as a guide for the researchers in selecting the appropriate platform that suits their research needs, and applications.

1. Introduction

Effective disease management and patient safety are the main goals of healthcare strategy. The two main pillars of medicine including now also personalized medicine are the clinical laboratory testing and hence, the selection of the optimum therapy (Getachew et al., 2019). Successful patient management and treatment in many clinical disorders including cancer and various infectious diseases are based nowadays on the detection and quantification of nucleic acids (NAs) of different nature's “such as deoxyribonucleic acid (DNA), ribonucleic acid (RNA), and microRNA (miRNA)” that are obtained from different sources such as whole blood, serum, plasma, and cells (Asha et al., 2019). Consequently, clinical laboratory medicine strives for the development of NAs biosensors that meet the rigorous demands of clinical laboratories including high sensitivity and specificity, with low cost, and short turnaround times (Hou et al., 2019).

NAs screening and quantification (sensing) are currently the cornerstones of prognosis and diagnosis of a multitude of clinical disorders diseases (Driscoll, 2007). Hence, a NAs biosensor could be defined as a device with biological NAs sensing elements connected to/or integrated within a transducer (Haupt and Mosbach, 2000; Kirsch et al., 2015; Mehrotra, 2016; Turner, 2013). Up-to-date there are several nanostructured materials that have been used as a novel emerging tools for designing NAs biosensors, such as carbon nanotubes (Yang et al., 2015a,b,c), quantum dots (QDs) (Martynenko et al., 2017), silica nanoparticles (Korzeniowska et al., 2013), gold nanoparticles (Shawky et al., 2010), and metal-organic frameworks (MOFs) (Zhou et al., 2018). In addition to, hybrid of different materials which enhance the behave of the biosensors (Carrasco, 2018; Chen et al., 2018; Liu et al., 2016; Shuai et al., 2017; Shuai et al., 2016a,b). MOFs, are prepared through self-assembly of metal ions and bridging organic ligands (Sheta et al., 2019a,b). MOFs have been explored extensively as sensors for the

* Corresponding author. National Research Centre, Inorganic Chemistry Department, 33- El-Behouth St., Dokki, 12311, Cairo, Egypt.
** Corresponding author. Center of Genomics, Helmy Institute, Zewail City of Science and Technology, October Gardens, 6th of October City, 12578, Giza, Egypt.
E-mail addresses: dr.sheta.nrc@gmail.com, sm.sheta@nrc.sci.eg (S.M. Sheta), sshawky@zewailcity.edu.eg (S.M. Shawky).

https://doi.org/10.1016/j.bios.2019.111451
Received 27 April 2019; Received in revised form 16 June 2019; Accepted 18 June 2019
Available online 24 June 2019
0956-5663/

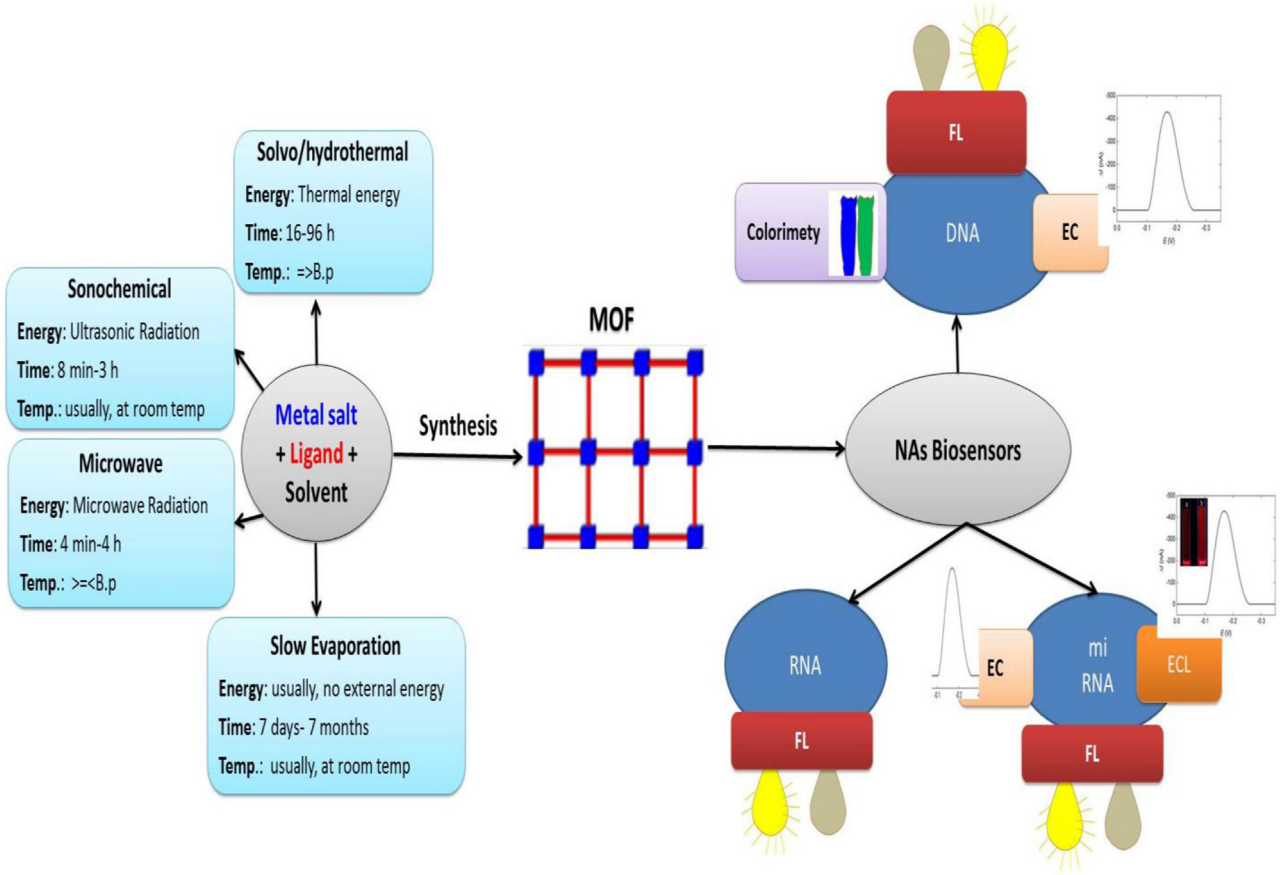

Scheme 1. Different synthetic methodologies of MOFs.

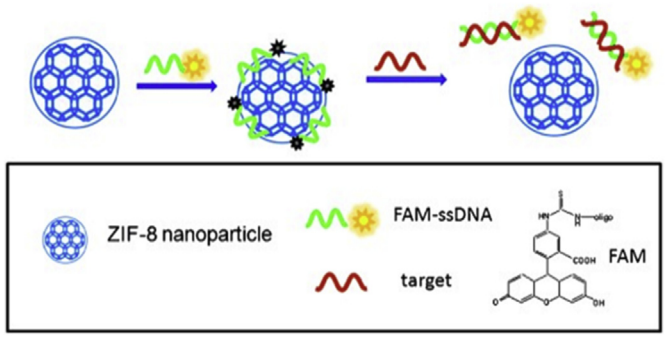

Fig. 1. A schematic (not to scale) illustrating fluorescence-enhanced nucleic acid detection using ZIF-8 NPs as a sensing platform (Reprinted with permission from ref. (Liu et al., 2012). Copyright 2012, Wiley).

detection of various analytes such as aromatic compounds (Takashima et al., 2011), oxygen (An et al., 2011; Xie et al., 2010), explosive chemicals (Lan et al., 2009; Pramanik et al., 2011), and amines (Qiu et al., 2008; Zou et al., 2009). Also have been successfully exploited in NAs detection such as DNA (Liu et al., 2012), RNA (Yang et al., 2015a,b,c), and miRNA (Wu et al., 2015).

Recently, among different nanomaterials, MOFs have received an increasing curiosity as NAs biosensors. Compared with other sensors (such as graphene, graphene Oxide, gold nanoparticles, and quantum dots), MOF-based NAs biosensors possess some potential advantages for biosensing: (1) MOFs' ligands usually contain a conjugated π-electron system that allows tight binding with the capture probe molecules via π-π stacking (Zhang et al., 2018); (2) MOFs providing a high loading capacity for the probe and resistance against probe degradation (He et al., 2014); (3) high surface area; (4) flexible porosity; (5) ease of organic functionality; (6) open metal sites in the skeleton that provides remarkable quenching properties and therefore enhance the detection sensitivity (Cheong and Moh, 2018; Ferey, 2008; Liu and Lu, 2007; Sheta et al., 2018); (7) MOFs are tailorable materials, because its properties can be adjusted just by changing the ratio of metal ions to ligands or other conditions; (8) good stability in different harsh environments (organic, aqueous, high temperatures, extreme pH conditions, etc.); (9) lower fabrication cost than bio-receptors; (10) the massive number of metal ions and organic linkers available have led to an unlimited number of new MOFs with designable and tailorable properties (Carrasco, 2018); (11) simple and easily one-pot synthesis (Dybtsev et al., 2004; Rubio-martinez et al., 2017; Wang et al., 2018; Xu and Kitagawa, 2018; Yuan et al., 2018), that could also post-synthesis modification, that enhances the specificity of molecular detection (Horcajada et al., 2012; Lei et al., 2014).

On the other hand, there are many disadvantages in using MOFs in NAs biosensors as lack of reusability in some cases; the low water stability of some types of MOFs that leads to the breakdown of the framework during the process of reusing; some types of MOFs aren't biocompatible; toxicity data of MOFs aren't sufficient, so the toxicity results dealing with MOFs are very scarce; sometimes, luminescent switch sensors (fluorescence) for the detection of NAs based on MOFs, have a low specificity due to "the unexpected targets may quench the fluorescence and result in false readings"; in some cases MOFs have a poor electrical conductivity that is a drawback in the designing of EC biosensors for NAs detection; there is no large-scale production of different types of MOFs which is the bottleneck for the development in practical applications.

MOFs synthesis is achieved through different methods, such as slow evaporation (Halper et al., 2006), solvothermal (Yaghi, 1997),

Table 1
MOFs based DNA fluorescent biosensors.

Meth. No.	TargetYear	Metal precursor/Ligand/Solvent/Modulator	Synthesis method	Structure	Q_E %	DT (min)	DR (nM)	LOD (pM)	Cross Reaction	Clinical Samples	Ref.
1	HIV-ssDNA/2012	$Zn(NO_3)_2$/2MI/H_2O	Slow Evaporation	1D	53	10	2.5–1000	N.D	_	_	Liu et al. (2012)
2	HIV-ssDNA/2013	$CuSO_4$/DTOA/H_2O	Sonochemical	2D	84.53	240	10–100	3000	_	_	Xi et al. (2013)
3	ssDNA/2014	$CdCl_2$/H_4L/DMF:H_2O	Solvothermal	3D	92	30	0–125	50	_	_	Wang et al. (2014a,b)
	ssDNA/2014	$Zn(NO_3)_2$/H_4L/DMF:H_2O	Solvothermal	3D	97	30	0–125	50	_	_	Wang et al. (2014a,b)
4	DNA/2015	$Fe(NO_3)_3$/H_2BDC/DMF	Solvothermal	3D	~100	3	0–5	10	_	_	Tian et al. (2015)
5	DNA/2016	$Gd(NO_3)_3$/TIA/DMF:H_2O	Solvothermal	3D	91	15	0–50	N.D.	_	_	Zhao et al. (2016a,b,c)
6	HIV-ssDNA/2014	Cr(NO3)3/TPA/H_2O/HF	Hydrothermal	3D	N.D	50	0.3–12	200	_	_	Guo et al. (2014)
7	HIV-ssDNA/2014	$Cr(NO_3)_3$/TPA/H_2O/HF	Hydrothermal	3D	88.81	42	0.1–14	73	_	_	Fang et al. (2014)
8	HIV-ssDNA/2014	$Zr_6O_4(OH)_4$/NH_2BDC/DMF	Solvothermal	3D	56	3	N.D	N.D	_	_	Zhang et al. (2014)
9	DNA/2017	$FeCl_3$/FA/H_2O	Microwave	3D	N.D	60	N.D	N.D	_	_	Mejia-ariza et al. (2017)
10	ssDNA/2017	$MnCl_2$/DMS/H_2O	Hydrothermal	2D	N.D	5	0.001–200	0.2	_	_	Song (2017)
11	HBV-ssDNA/2014	$CuSO_4$/DTOA/H_2O	Sonochemical	2D	85	40	1–10	870	tested	_	Ye et al. (2014)
	HIV-ssDNA/2014	$CuSO_4$/DTOA/H_2O	Sonochemical	2D	91.1	40	1–10	220	tested	_	Ye et al. (2014)
12	H1N1, H5N1 DNA/2015	$Cu(NO_3)_2$/TCPP/DMF:ETOH/PVP	Solvothermal	2D	89	5	0–5	20	_	_	Zhao et al. (2015a,b)
13	HIV-dsDNA/2014	$CuSO_4$/DTOA/H_2O	Sonochemical	2D	81	180	4–200	1300	_	_	Chen et al. (2013)
14	HIV-dsDNA/2015	$CuSO_4$/H_3CmdrpBr,dps/H_2O/NaOH	Hydrothermal	3D	65	90	10–50	196	tested	_	Yang et al. (2015)
15	HIV-dsDNA/2016	$Cu(NO_3)_2$/H_2dcbbBr/H_2O	Hydrothermal	2D	62	90	1–120	1420	_	_	Zhao et al. (2016)
16	HIV-dsDNA/2016	$Zn(NO_3)_2$/Cbdcp,bpe/DMF/Aspirin	Solvothermal	2D	73	80	1–80	10	_	_	Zhao et al. (2016)
17	DNA/2016	$Fe(NO_3)_3$/FA/DMF	Solvothermal	3D	~100	30	3–150	1000	_	Sp. serum	Tan et al. (2016)
18	p53 gene/2018	$ZrCl_4$/TCPP,BA/DMF	Solvothermal	3D	98.84	5	0.01–10	5	tested	Sp. serum	Huang et al. (2018)
	BRCA1 gene/2018	$ZrCl_4$/TCPP,BA/DMF	Solvothermal	3D	95.5	5	0.001–5	1	tested	_	Huang et al. (2018)

*All assays in the table has a high specificity to single base mismatched DNA; Meth. No.: method number; Q_E: quenching efficiency; DR: detection range; DT: detection time; LOD: limit of detection; N.D.: not detected or not mentioned in the literature; sp. serum: spiked serum; 2MI: 2-methylimidazole; DTOA: dithiooxamide; H_4L: bis-(3,5-dicarboxy-phenyl)terephthalamide; H_2BDC: 1,4-benzenedicarboxylic acid; TIA: 5-triazoleisopthalic acid; TPA: terephtalic acid; NH_2-BDC: 2-amino-1,4- benzenedicarboxylic acid; DMF: N'N-dimethylform-amide; FA: fumaric acid; DMS: 2,2-dimethylsuccinate; TCPP: tetrakis (4-carboxyphenyl) porphyrin; ETOH: ethanol; PVP: polyvinylpyrrolidone; H_3CmdrpBr: N-carboxymethyl-3,5-dicarboxylpyridinium bromide; dps: 4,4′-dipyridyl sulfide; H_2dcbbBr: 1-(3,5-dicarboxybenzyl)-4,4′-bipyridinium bromide; Cbdcp: N-(4-carboxybenzyl)-(3,5-dicarboxyl)pyridinium); bpe: trans-1,2-bis(4-pyridyl)ethylene; BA: benzoic acid.

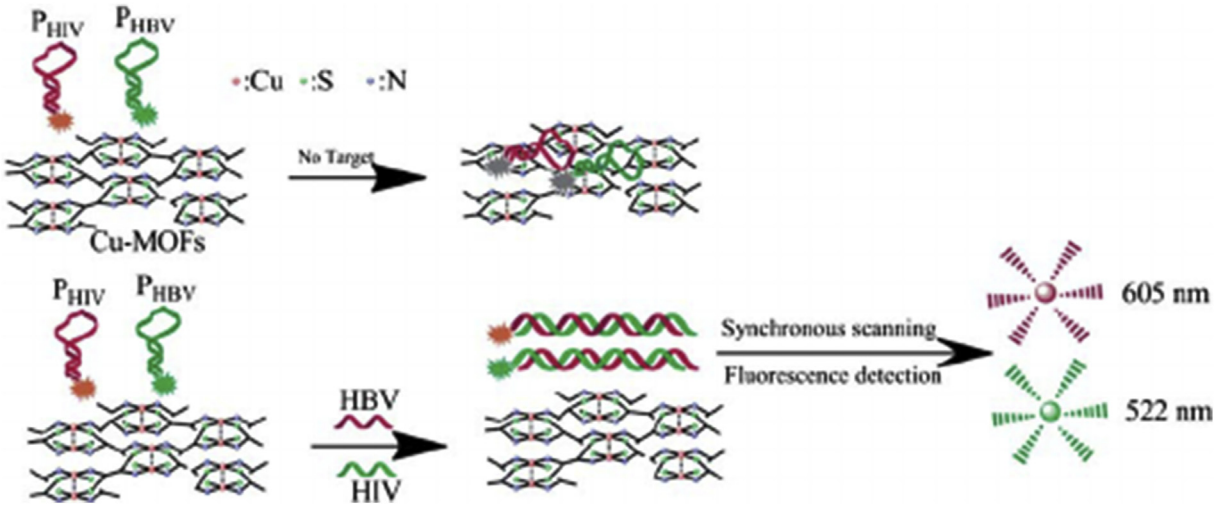

Fig. 2. The principle of simultaneous detection of T1 and T2. (Reprinted with permission from ref. (Ye et al., 2014). Copyright 2014, Royal Society of Chemistry).

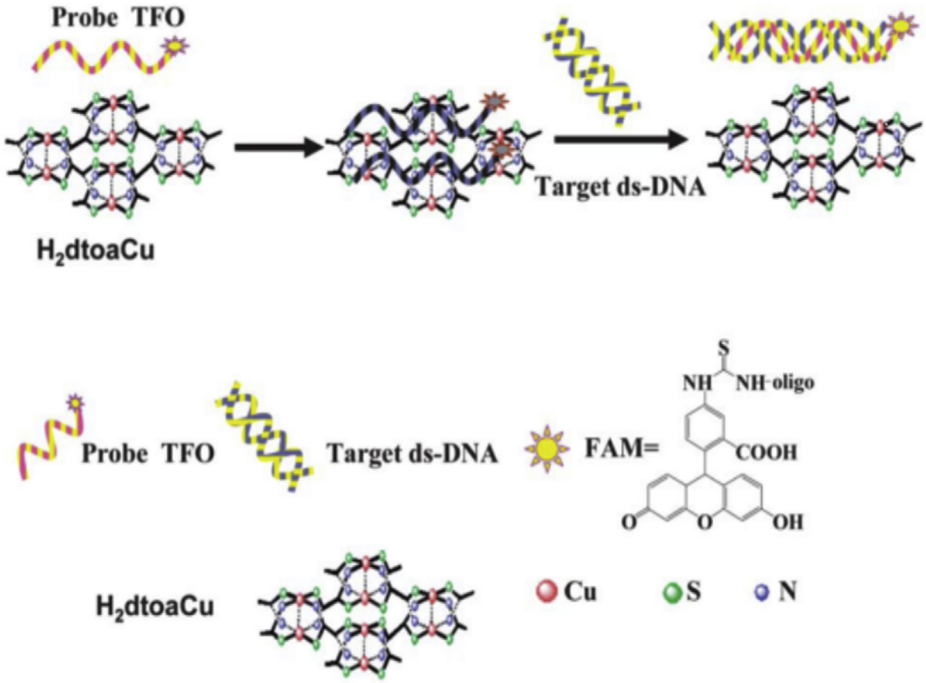

Fig. 3. Mechanism for the ds-DNA fluorescent biosensor based on MOF. (Reprinted with permission from ref. (Chen et al., 2013). Copyright 2013, Royal Society of Chemistry).

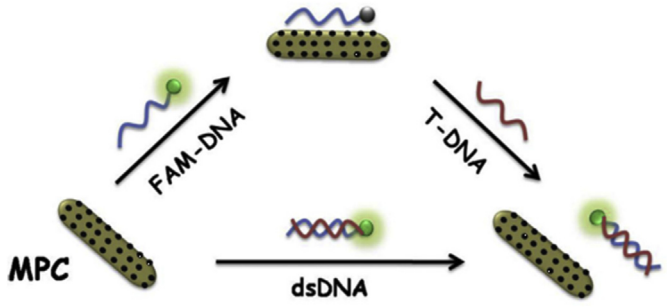

Fig. 4. Schematic illustration of MPC as a sensing platform for DNA fluorescent detection. (Reprinted with permission from ref. (Tan et al., 2016). Copyright 2016, Elsevier).

electrochemistry (Mueller et al., 2011), hydrothermal (Crane et al., 2015), microwave (Jhung et al., 2005), sonochemical (Kim et al., 2011), mechanochemistry (Garay et al., 2007), spray dryer (Imaz et al., 2013), flow cytometry (Rubio-martinez et al., 2016), and others (Rubio-martinez et al., 2017). Some synthetic techniques of MOFs gradually emerged, such as microwave-ultrasound-assisted synthesis method (Jia et al., 2013), ionic liquid microemulsions (Zheng et al., 2017), continuous flow production (Rubio-martinez et al., 2014), surfactant-mediated hydrothermal syntheses (Yuan et al., 2011), and modulator-assisted synthesis method (Pham et al., 2011). Nanotechnology is a rapidly evolving field, whose integration in MOFs preparation leads to a positive impact on the synthesis and detection methods used for nucleic acids biosensors (Yuan et al., 2018). The design of NAs biosensors based on MOF is highly dependent on the detection method such as fluorescence (FL), electrochemistry (EC), electrochemiluminescence (ECL) and colorimetry.

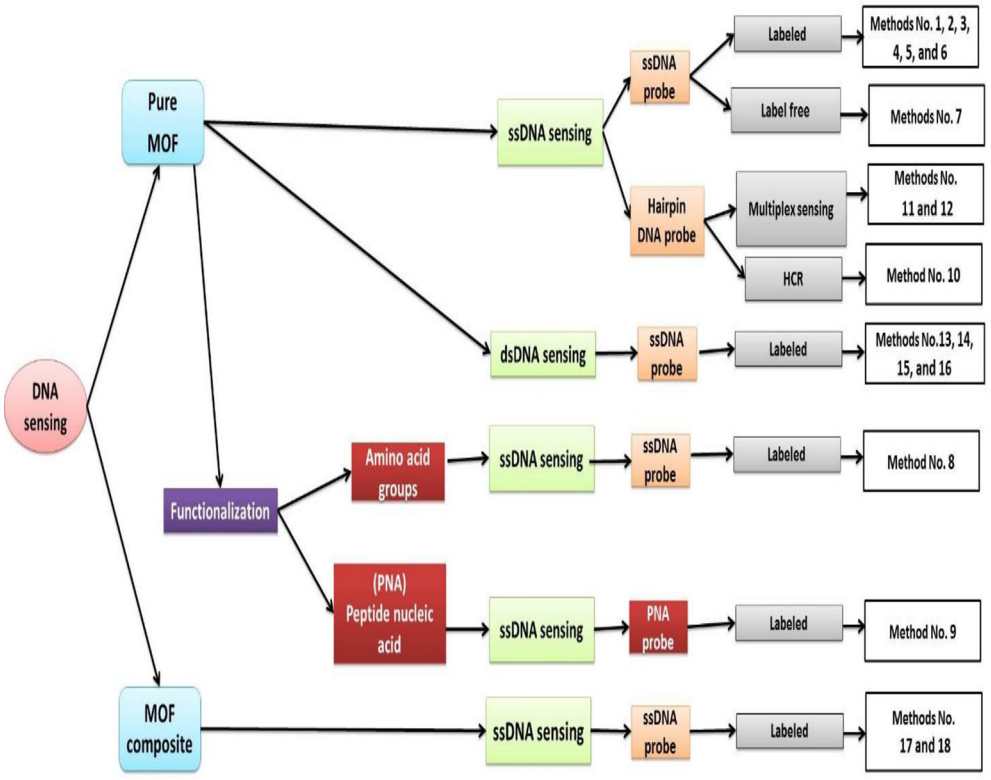

Scheme 2. Schematic representation of all mentioned DNA sensing techniques.

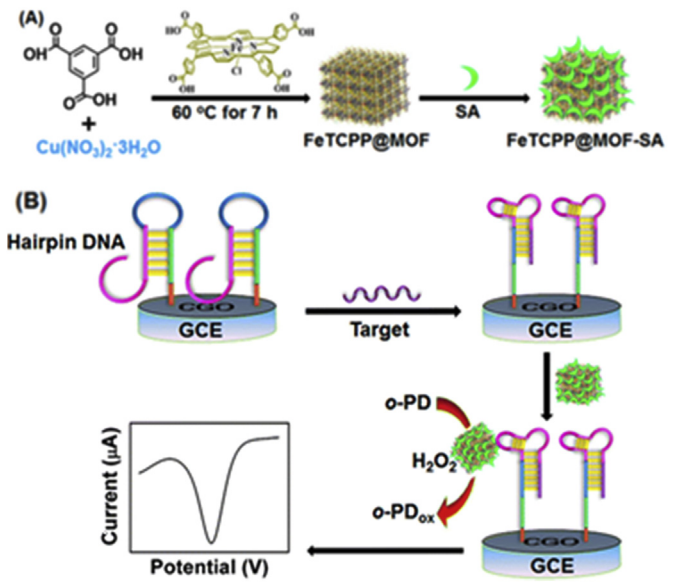

Fig. 5. (A) Synthesis of FeTCPP@MOF-SA composite and **(B)** Electrochemical DNA sensing via allosteric switch of hairpin DNA. (Reprinted with permission from ref. (Ling et al., 2015b). Copyright 2015,American chemical society).

This review will discuss the nucleic acids biosensors development based on the popular MOFs fluorescent, electrical, and colorimetric techniques. Additionally, we will highlight the challenges and the future prospects of introducing NAs biosensors based on MOFs in clinical diagnostics. To the best our knowledge, this is the first report to discuss a broad perspective of DNA, RNA, and miRNA sensing starting from MOFs synthesis to the various clinical applications.

2. Synthetic methodologies of MOFs

The MOFs synthesis methodologies are affecting by different factors and many experimental parameters based on the final properties and MOFs structures. As example, the presence of additives like modulator is added to adjust the particle size, pores and consequently the structure, type of linkers and organic ligand, and the type of metal, etc. (Dey and Kundu, 2014a, 2014b; Karina et al., 2017; Stock and Biswas, 2012). In addition, the type of the solvent or mixture of solvents is very important to overcome the different solubility of the starting materials and also to control the activation energy (Seetharaj et al., 2019). The main MOFs synthesis methodologies used through this review shown in Scheme 1. These methods are slow evaporation (Halper et al., 2006; Tranchemontagne et al., 2008; Yoo et al., 2011), solvothermal/hydrothermal (Butova et al., 2016; Crane et al., 2015; Dey and Kundu, 2014b; Mckinstry et al., 2016; Pachfule et al., 2011), microwave (Hindelang et al., 2012; Klinowski and Paz, 2011; Liang and Alessandro, 2013; Liang et al., 2013; Seo et al., 2009), and sonochemical method (Carson et al., 2011; Dharmarathna et al., 2012) depending on the main parameters such as energy, time, and quality of the MOF synthetic methodologies.

Generally, the synthesized MOFs can be characterized using different analytical techniques and equipment's such as single crystal X-ray spectroscopy, ^{1}H-NMR, ^{13}C-NMR, mass spectrometry, elemental analysis, Fourier transform-infrared (FT-IR), UV–vis, X-ray diffraction (XRD), X-ray photoelectron spectroscopy (XPS), field emission scanning electron microscopy (FE-SEM) combined with element mapping by spatially resolved energy-dispersive X-ray spectroscopy (EDX), high-resolution transmission electron microscope (HR-TEM), thermo-gravimetric analysis (TGA), etc. (Howarth et al., 2017; Lucier et al., 2018).

3. DNA sensing based on MOFs

MOFs based DNA biosensors are mainly carried out via fluorescence, electrochemistry and/or colorimetric techniques will be

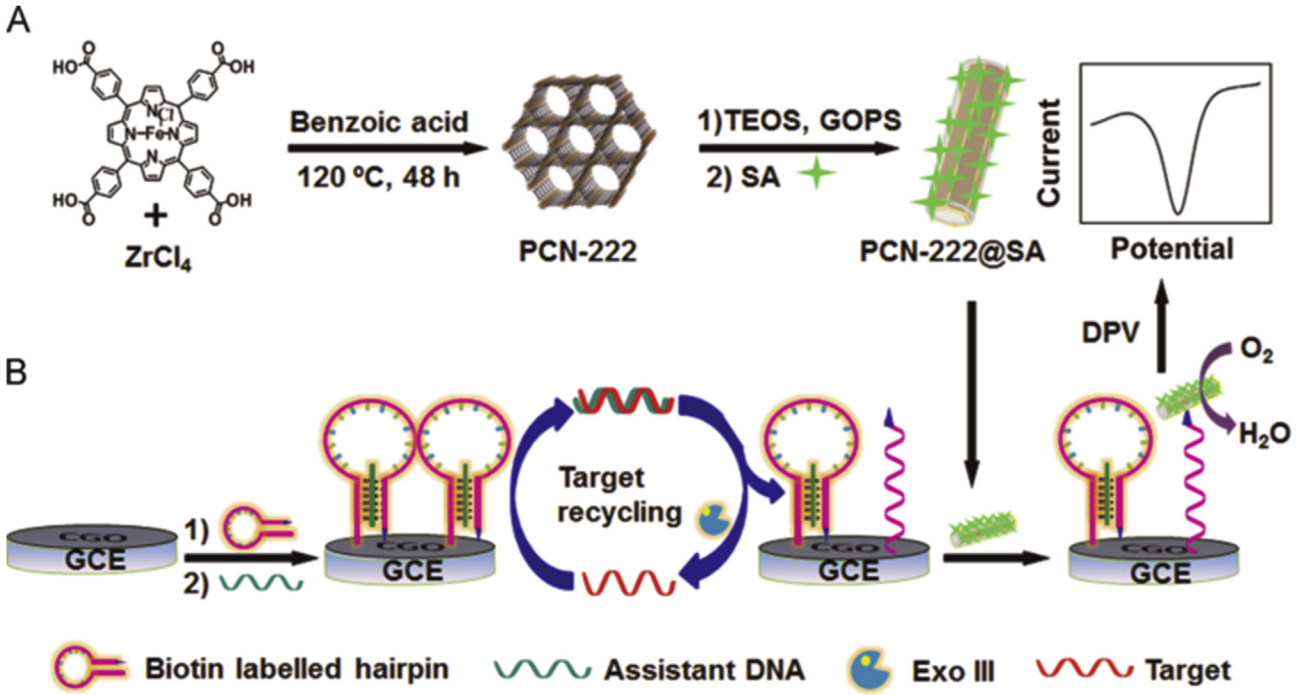

Fig. 6. (A) Synthesis of PCN-222@SA composite, and **(B)** electrochemical strategy coupling with target recycling amplification for DNA sensing. (Reprinted with permission from ref. (Ling et al., 2015a). Copyright 2015, Elsevier).

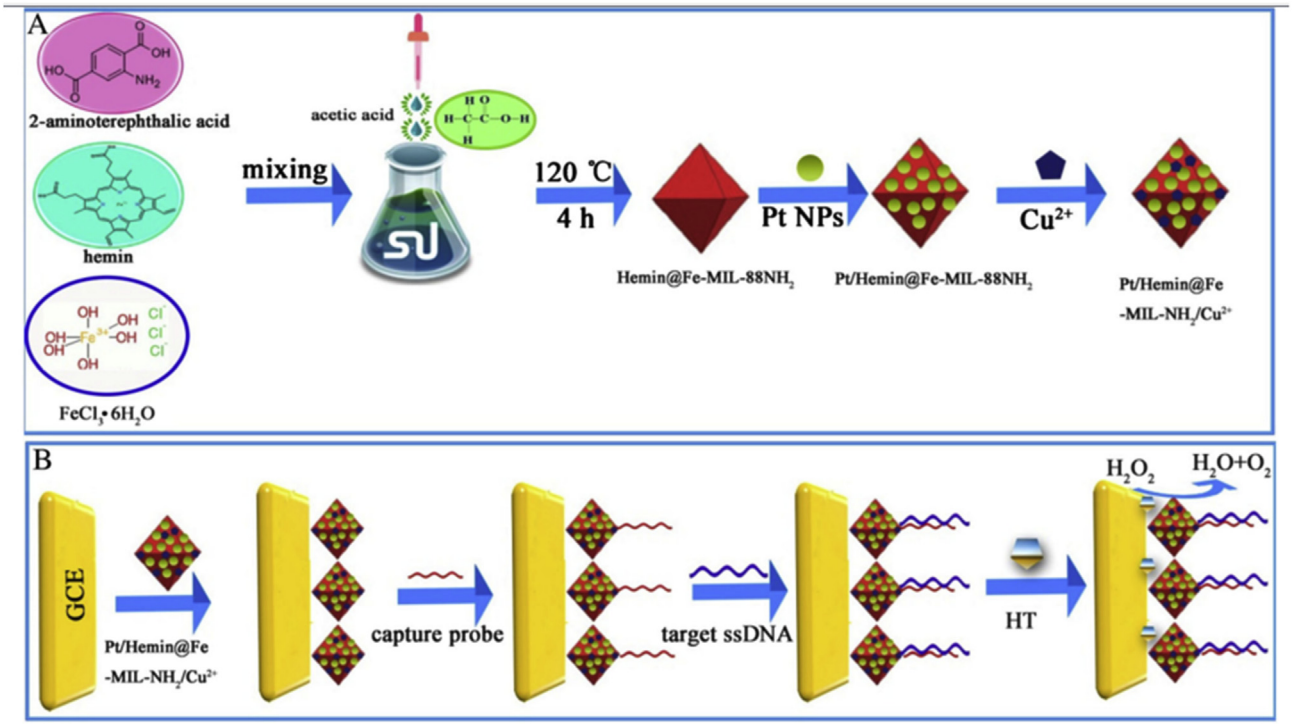

Fig. 7. (A) The preparation process of Pt/Hemin@Fe-MIL-88NH_2/Cu^{2+}, **(B)** Schematic representation of the electrochemical DNA sensor. (Reprinted with permission from ref. (Yuan et al., 2017). Copyright 2017, Springer).

discussed in details in this section.

3.1. Fluorescence technique

(Liu et al., 2012) are the first who exploited the MOFs chemical and physical properties in DNA sensing. A subclass of MOFs called zimidazolate framework-8 nanoparticles (ZIFNPs), have been synthesized, and used for the detection of human immunodeficiency virus-single strand DNA (HIV-ssDNA) based on fluorescence quenching phenomenon. FAM-labeled ssDNA probe specific to the HIV-ssDNA exhibits high fluorescence in the absence of ZIFNPs. However, when binds with the ZIFNPs by electrostatic and π–π interactions fluorescence quenching occurs. By the addition of the HIV-ssDNA target, hybridization of the FAM-labeled probe with target occurs leading to its

Table 2
MOFs based electrochemical DNA biosensors.

Meth. No.	Target/ Year	Metal Precursor/Ligand/ Solvent/Modulator	Composite	Synthesis	Electrode		Immob.Method	DM	DT(h)	DR	LOD (fM)	Cross Reactivity	Clinical Samples	Ref.
1	DNA/2015	$Cu(NO_3)_2$/TCPP/ DMF:ETOH/H_3BTC	FeTCPP@MOF	Solvothermal	GCE		Covalent	CV,DPV	2	10 fM-10 nM	0.48	–	Sp. serum	Ling et al. (2015b)
2	DNA/2015	$ZrCl_4$/TCPP(Fe)/DMF/BA	FeTCPP@MOF	Solvothermal	GCE		Covalent	CV,DPV	2	10 fM-100 nM	0.29	–	Sp. serum	Ling et al. (2015a)
3	FGFR3/ 2016	$FeCl_3$/2ATPA/DMF/AcOH	hemin-MOF/ PtNPs	Solvothermal	GCE/rGO-TEPA /AuNP/SA		SA-Biotin link	CV,EIS	4	0.1 fM-1 nM	0.033	–	Sp. serum	Yu et al. (2016)
4	ADRB1/ 2017	$FeCl_3$/2ATPA/DMF/AcOH	Pt/hemin@ MOF/Cu^{2+}	Solvothermal	GCE/(Pt/Hemin@Fe-MIL-88NH_2/Cu^{2+})		Covalent	CV	2	1 fM–10 nM	0.21	–	Sp. serum	Yuan et al. (2017)

***All assays in table has a high specificity to single base mismatched DNA; Immob.:** immobilization; **DM:** detection method; **CV:** cyclic voltammetry; **EIS:** electrochemical impedance spectroscopy; **DPV:** differential pulse voltammetry; **2ATPA:** 2-aminoterephtalic acid; **AcOH:** acetic acid; **PdNPs:** Palladium nanoparticles; **rGO-TEPA:** Reduced grapheme oxide tetraethylene pentamine; **FGFR3:** fibroblast growth factor receptor 3 gene; **ADRB1:** adrenergic receptor gene; **SA:** streptavidine; **PEI:** Polyethyleneimine; **FeTCPP:** iron(III) meso-5,10,15,20-tetrakis(4-carboxyphenyl) porphyrin chloride.

release from the ZIFNPs surface, and fluorescence recovery as shown in Fig. 1. The authors declared that this platform has a linear range of 2.5–1000 nM, with a high specificity down to single-based mismatch detection (Fig. 1). However, this platform sensitivity suffers from low sensitivity due to its low quenching efficiency (53%).

Increasing sensitivity has been achieved by using, a 2D MOF, N,N′-bis(2-hydroxy-ethyl) dithiooxamidatocopper (II) [$Cu(H_2dtoa)$] (Xi et al., 2013), which has been used for the detection of HIV ssDNA, utilizing the intrinsic quenching properties of Cu-MOF. When human immunodeficiency virus (HIV) specific probe labeled with FAM dye added to the prepared MOF, a hydrophobic and π-stacking interaction takes place between them, leading to the dye quenching. Upon addition of the target (HIV ssDNA), hybridization with the FAM-labeled probe takes place forming a rigid ds-DNA structure that is released from the MOF, leading to fluorescence recovery. Although, this approach provided target detection up to 3 nM and showed high selectivity and specificity with single base mismatch detection, thus it is time consuming 4 h, and required complicated pretreatment processes to generate ssDNA prior to analysis compared with the other sensing technique. In the same context, Cd-MOF and Zn-MOF, have shown high sensitivity and selectivity when used as quenchers for FAM-labeled probes (Wang et al., 2014a,b), with a limit of detection (LOD) of 0.05 nM. Table 1, summarizes a comparison among most of the published reports related to MOFs based DNA fluorescent biosensors.

The synergy effect of the metal center (iron) and the organic linker have been exploited in iron-based MOF nanorods that greatly enhance the overall fluorescence. Iron-based MIL-88B MOF nanorods (Tian et al., 2015) have been used as a high-efficient sensing platform for fluorescence DNA detection, with LOD up to 10 pM, and the single point mutation discrimination. In addition, this biosensor is cheap, easy, rapid, and takes only 4 min for the whole "mix-and-detect" process. However, it has not been tested yet on real clinical samples.

Another property/type of MOF is the pure color of lanthanides–MOFs and its intrinsic luminescence due to f-f transitions, make these MOFs remarkable luminescent biosensors (Zhao et al., 2015a,b). Consequently, gadolinium-based MOF that was prepared solvothermally, has the ability to efficiently detect the presence of the target DNA complementary sequence (Zhao et al., 2016a,b,c). The linearity of this platform was shown to be from 0 to 50 nM, with high specificity up to one base pair mismatch DNA sequence. However, it wasn't tested on real clinical samples.

MIL-101 MOF has been used as a fluorescence anisotropy (FA) amplifier for the detection of HIV-ssDNA target (Guo et al., 2014). Adsorption of FAM-labeled ssDNA probe onto MIL-101 surface leads to restriction of the fluorophore rotation and exhibiting a large FA value in the absence of the target, 0.32. On the other hand, in the presence of the DNA target, a ds-DNA is formed between the FAM-labeled probe and the DNA target, away from the MOF surface resulting in lowering the FA value, 0.15. Based on this method, HIV-ssDNA can be detected up to 0.2 nM, and this assay assumed that MIL-101 is an effective fluorescence anisotropic enhancement material. However, this method isn't effective for the point of care (POC) as anisotropy based detection method and is not practical in clinical laboratories. Additionally, the process of fluorescent dye labeling for DNA probes is a very tedious and expensive process. So, dependence on the label-free probe is an urgent need. Consequently, MIL-101 has been used as DNA biosensor using dye free probe (Fang et al., 2014). A labeled free probe and syber green (SG) fluorescent dye complex was adsorbed to the MOF via π–π stacking and electrostatic interactions and quenched the fluorescence of the SG dye. When the target HIV-ssDNA is added, hybridization occurred between the probe and the target forming rigid ds-DNA. The formed ds-DNA takes the SG dye away from MOF surface and this is accompanied by fluorescence recovery. This method has a sensitivity over the range from 0.1 to 14 nM with a LOD of 73 pM and the specificity can reach to one-base mismatch, with overall 30 min for the detection time.

To achieve high selective and rapid detective biosensors platforms,

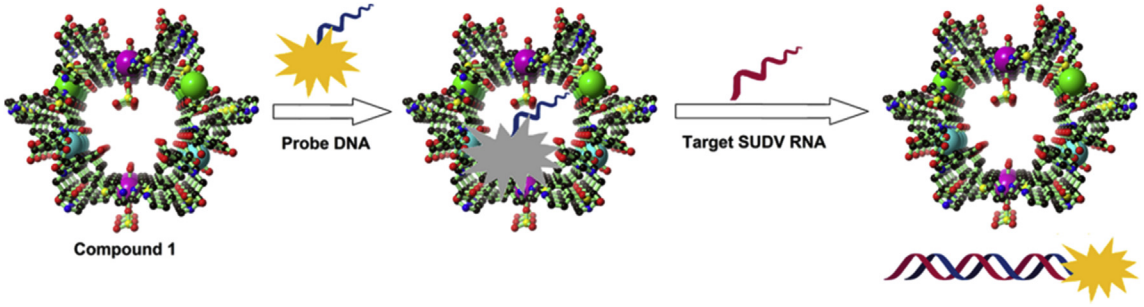

Fig. 8. Proposed mechanism for the detection of target SUDV RNA sequences based on a fluorescent biosensor formed from compound 1 and fluorophore-labeled probe DNA. (Reprinted with permission from ref. (Yang et al., 2015a,b,c). Copyright 2015, American chemical society).

syntheses of different MOFs that functionalized with different groups have been reported. The addition of amino groups to the UiO-66 platform enhanced the hybridization between the target and the FAM-labeled probe with selectivity up to one base pair mismatch recognizing due to the recovery of the fluorescence up to 70%. This design was utilized in HIV-ssDNA detection (Zhang et al., 2014). Moreover, surface functionalization of iron-MOF, MIL-88A (Mejia-ariza et al., 2017), has been utilized for DNA detection, quantification, and distinguishing single-base mismatched. In this strategy, biotin-labeled peptide nucleic acid (PNA) specific to the DNA target has interacted with streptavidin-coated MIL-88A MOF particles through the firm biotin-streptavidin link. The target-PNA hybridization has been confirmed by confocal microscopy and flow cytometry and shown high specificity and sensitivity.

To amplify the fluorescence signal obviously, hybridization chain reaction (HCR) strategy has been compiled with MOFs as a highly sensitive, specific and rapid NAs biosensor (Song, 2017). It is based on two hairpin DNA probes each of which is modified with TAMRA fluorophore. With the mixing of probes with Mn-MOF nanosheets, the two probes are adsorbed on its surface and their fluorescence is obviously quenched. Upon the target ssDNA addition, the two probes hairpin structures are opened due to their complementary with the target DNA, and the HCR is initiated between the two probes, and the latter are sequentially open to assemble into a long double strand DNA (dsDNA) with collected fluorophores. The fluorescence detected is an indication of the target concentration over the range from 1 to 200 pM with a LOD equals 0.2 pM. The whole reaction takes only 5 min. However, it wasn't tested for cross-reactivity and wasn't applied to real human samples or even spiked serum samples.

Molecular beacons (MBs) are probes with a stem-looped structure with a fluorescent dye and a quencher that are attached to their 5 and 3 ends, respectively leading to the dye quenching due to their close proximity on the probe. Upon binding with the target nucleic acid, the MB hairpin structure opens and hybridize with the target restoring the dye fluorescence, indicating the target presence. MBs are highly sensitive and specific up to discriminating one base mismatch and are the probe of choice in multiplexing detection (Kim et al., 2008). In an interesting study (Ye et al., 2014), MBs probes specific to HIV and HBV have been compiled with MOF, Cu(H_2dtoa), onto which the probes are adsorbed on the MOF surface. The adsorption is accompanied by fluorescence quenching which is recovered with the target addition as shown in Fig. 2. In this study, the authors have utilized the known characteristics of the MBs probes in specific detection of the nucleic acids, with the intrinsic properties of the MOFs as quenchers. Depending on this method, HIV and HBV can be detected up to 0.22 nM and 0.87 nM, respectively. Moreover, this platform is considered to be the first MOF based multiplexing NAs detection.

A similar strategy was pursued in the simultaneous detection of the Influenza A virus subtype H5N1 gene (T1) and subtype H1N1 gene (T2) (Zhao et al., 2015a,b). This method used a bottom-up method, a surfactant-assisted synthetic method, to produce uniform ultrathin 2D Cu-MOF nanosheets and polyvinylpyrrolidone (PVP) was used as a surfactant during the preparation. This 2D structure has enhanced the LOD up to 20 pM. The main drawback of this method and all the above methods is the cumbersome pretreatment processes required for target-ssDNA preparation prior to use.

On the other hand, MOF-Cu(H_2dtoa) has been developed as a sensitive and simple biosensor for double-stranded DNA (dsDNA) detection (Chen et al., 2013). The method is based on free triplex-forming oligonucleotide (TFO) probe labeled with FAM at 5′ end. It is quenched by the above mentioned MOF through stacking π-electron systems of the bridging ligand dithiooxamide and the metal center Cu^{2+} that results in photoinduced electron transfer (PET) process and FAM fluorescence quenched in sample with a synthetic target of HIV-dsDNA was added to Cu(H_2dtoa)/TFO, so the FAM fluorescence was maintained due to the formation of triplex form through hoogsteen or reverse hoogsteen hydrogen bonding between the TFO probe and the double strands of HIV. Then, a relationship between the HIV-dsDNA concentration and the intensity of the fluorescence recovery was studied for quantitative measurement. This method is sensitive over the linear range of 4–200 nM with a LOD of 1.3 nM (Fig. 3). However, it takes a long detection time, 3h. A water-stable Cu-MOF, which has a distinct response to ss and ds DNA has been used as quenching substrate for the detection of HIV-1 dsDNA with LOD of 196 pM and one base pair mismatch distinguishing and is shown no cross-reactivity with Sudan virus RNA (Yang et al., 2015a,b,c). However, it takes a long detection time and wasn't tested for clinical samples as shown in Table 1.

In a comparison study of the MOF structure dimensions (Zhao et al., 2016a,b,c), three different polymorphic compounds were synthesized; the first was a 1D chain, while the second was 2D layer and the third was first/second co-crystal Cu-MOF structure and the three structures were tested as FAM quenchers. It was shown that 2D Cu-MOF (the network structure of the second compound) is more effective in HIV-dsDNA (LOD 1.42 nM) as the 2D layer has a higher exposure surface with functional groups to form interactions with probe ss-DNA and so better hybridization with the target, reflected in enhancing the sensitivity. Moreover, the effectiveness of the 2D MOF as DNA biosensors over the 1D and 3D structures has been confirmed in a study used 2D Zn-MOF that reached 10 pM in HIV dsDNA (Zhao et al., 2016a,b,c). The main drawback of this method is that it wasn't tested on real clinical samples or spiked serum samples.

In addition to pure MOFs, nanohybrids have also been used in designing DNA biosensors. Iron–MOFs (MIL-88A) was used as a precursor for the synthesis of magnetic porous carbon (MPC) nanocomposite, via a one-pot thermolysis method (Tan et al., 2016). The prepared MPC has provided a sensitivity for DNA detection up to 1 nM, as shown in Fig. 4. It was successfully applied to spiked fetal bovine serum (FBS) samples. However, this method takes 30 min as the detection time.

Also, a highly sensitive, selective, rapid, and cost-effective biosensor was developed based on nanohybrid (Huang et al., 2018). MOF@AuNP@GO nanohybrid has been synthesized and compared with MOF@GO and MOF@AuNP in detecting p53 gene and BRCA1 genes as

Table 3
MOF based RNA fluorescent biosensors.

Meth. No.	Target/Year	Metal precursor/Ligand/Solvent/Modulator	Synthesis Method	Structure	Q_E %	DT(min)	DR (nM)	LOD (PM)	Cross Reactivity	Clinical Samples	Ref.
1	SUDV RNA/2015	$CuSO_4/H_3CmdcpBr$,dps/H_2O/NaOH	Hydrothermal	3D	76	30	10–50	73	tested	–	Yang et al. (2015)
2	SUDV RNA/2017	$La(NO_3)_3/H_3CmdcpBr$/MeOH/NaOH	Slow Evaporation	3D	70.2 ± 5.3	30 ± 5	0–50	112	–	–	Yang et al. (2017)
	SUDV RNA/2017	$La(NO_3)_3/H_3CbdcpBr/H_2O$/NaOH	Hydrothermal	2D	57.3 ± 5.3	18 ± 2	0–50	67	–	–	Yang et al. (2017)
3	EBOLV RNA/2016	$Dy(NO_3)_3/H_3CmdcpBr$ /H_2O	Hydrothermal	3D	60	120	5–50	160	–	–	Qin et al. (2016)
4	DENV RNA/2018	$CuSO_4$/bpe,$H_3DcbcpBr/H_2O$	Hydrothermal	3D	92	36	1–60	332	–	–	Xie et al. (2018)
	ZIKV RNA/2018	$CuSO_4$/bpe,$H_3DcbcpBr/H_2O$	Hydrothermal	3D	92	2	0.5–70	192	–	–	Xie et al. (2018)
	DENV, ZIKA RNA/2018	$CuSO_4$/bpe,$H_3DcbcpBr/H_2O$	Hydrothermal	3D	*82, 92	N.D	0–60	*184, 121	tested	–	Xie et al. (2018)

* **DENV, ZIKV, **All assays in table has a high specificity to single base mismatched RNA; H_3CmdcpBr**: N-carboxymethyl-3,5- dicarboxylpyridinium bromide; H_3CbdcpBr**: N-(4-carboxybenzyl)-3,5-dicarboxylpyridinium bromide; H_3DcbcpBr**: N-(3,5-dicarboxylbenzyl)-(3-carboxyl) pyridinium bromide; **SUDV**: sudan virus; **EBOLV**: Ebola virus; **DENV**: Dengue virus; **ZIKAV**: Zika virus.

cancer biomarkers. The results of the comparison showed that the hybrid of MOF@AuNP@GO is more effective than others, and is sensitive in detecting p53 and BRCA1 genes with LODs of 5 pM and 1 pM, respectively. This assay was successfully applied to spiked serum samples.

Table 1 represents all MOFs based DNA fluorescent biosensors mentioned in this review and summarized as well in Scheme 2. Through the Table, it is deduced that all biosensors haven't been applied to real human clinical samples. Also, methods number 11 and 14 were tested only on spiked serum samples. While all the other methods were tested only on the synthetic target. Also, all methods, except methods 11, 14 and 18, weren't tested for cross-reactivity. As mentioned above, dsDNA detection is better than ssDNA detection, due to the complicated pretreatment processes to prepare the target-ssDNA prior to use. However, dsDNA sensing requires a long detection time, up to 180 min. In addition, 2D MOF structure has better performance than 3D, because the 2D structure has a larger surface area subjected to the target that means better hybridization and so, better sensitivity and each method has its merits and demerits.

To the best of our knowledge, there isn't an optimum technique for designing new DNA biosensors. Moreover, the best method varies according to your target, for example, if you design a new DNA biosensor for simultaneous detection, so the methods number 4, 8, 10, 12, and 18 are remarkable for future planning researches. While, if you develop an ultrasensitive biosensor, methods number 10 and 18 are significant.

3.2. Electrochemical technique

Electrochemical sensor one of the common detection methods for DNA, and it has been attracted more attention due to its high sensitivity, rapid response, simplicity, and portability (Chidambaram and Stylianou, 2018; Fan et al., 2003; Farjami et al., 2011; Xiao et al., 2007). The immobilization method of the probe onto the modified electrode surface plays an important role in the overall performance of the NAs biosensors (Marrazza et al., 1999; Wang, 2000). Most of MOFs based electrochemical NAs biosensors consist mainly of two units, capture unit (modified electrode) and signal unit (signal probe). MOF usually represents the signal unit due to its mimetic catalysis properties that magnify the electrochemical signal. Most types of MOFs have a low electrical conductivity that is the barrier for broad using of pure MOFs in electrochemical NAs biosensors. Therefore, MOF composites are usually used in EC biosensors to solve the conductivity problem.

The nanocomposite of porphyrin-encapsulated MOF, FeTCPP@HKUST-1, treated with streptavidin (SA) was used as a signal unit or a signal probe to prepare a highly sensitive EC DNA biosensor (Ling et al., 2015b). The prepared nanocomposite is a good electrochemical indicator for signal readout due to its ability to catalyze the oxidation reaction of o-phenylenediamine (o-PD) with H_2O_2. The capture probe, hairpin DNA, immobilized on the glassy carbon electrode (GCE), considered as the capture unit. With introducing the target ssDNA, the hairpin probe DNA was unfolded and subsequently, a free SA-aptamer was formed. With the signal unit addition, the free aptamer interacts with the streptavidin, and bring FeTCPP@MOF-SA to the electrode surface. Then, the generated signals are enhanced as shown in Fig. 5. These electrochemical signals were measured by cyclic voltammetry (CV) and differential pulse voltammetry (DPV) techniques. In this assay, the LOD was 0.48 fM. This method could remarkably discriminate target DNA even from single-base mismatched oligonucleotide and good feasibility in complex spiked serum matrixes.

Another porous coordination network (PCN) composite of zirconium-porphyrin MOF (PCN-222), treated with streptavidin (SA) was used as a signal probe to prepare a highly sensitive and selective EC biosensor (Ling et al., 2015a). PCN-222 composite has the ability to electrocatalyse O_2 reduction and this property was exploited to greatly enhance the electrochemical signal readout. The capture unit can be represented by the probe, biotin-labeled triple-helix, immobilized on the GCE. On the addition of the target ssDNA, the assistant DNA in

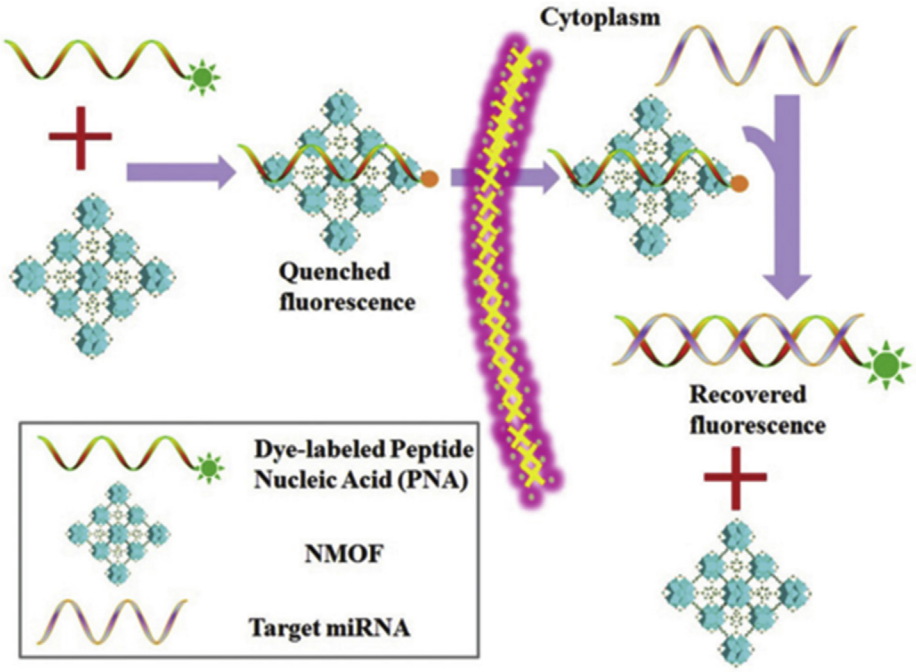

Fig. 9. The PANMOF- based miRNA sensing mechanism. (Reprinted with permission from ref (Wu et al., 2015).. Copyright 2015, Royal society of chemistry).

triple-helix will hybridize with target DNA. This leads to the activation of the end biotin for caching the signal nanoprobe, PCN-222@SA, via a streptavidin-biotin link, and thus, the signal probe is attached with the electrode surface (Fig. 6). Integrating with DNA recycling amplification of exonuclease III, a LOD reached up to 0.29 fM. Moreover, this method approved high specificity when successfully applied to detect DNA in complex spiked serum samples.

A similar strategy has pursued the detection of FGFR-3 mutation gene, a useful biomarker for early non-invasive prenatal diagnosis (NIPD) of achondroplasia (Yu et al., 2016). In this biosensor, the signal unit is represented by a composite of Fe-MIL-88, hemin, PtNPs, signal probe (SP) and bovine serum albumin (BSA). While the capture unit is represented by GCE modified by reduced graphene oxide-tetraethylenepentamine (rGO-TEPA), gold nanoparticles (AuNPs), streptavidin and biotin-modified ssDNA probe. The addition of the target ssDNA is sensed by hybridization with the capture probe. With the addition of hydrogen peroxide and the prepared signal unit to the solution, an intrinsic increase of the electrical signal is observed due to hemin-MOFs/PtNPs nanomaterial has a unique ability to catalyze H_2O_2 reduction as well as excellent conductivity. Also, in the same study, gold nanoparticles were tested as an alternative to PtNPs. But the results showed that using of PtNPs is highly effective than AuNPs. Based on using PtNPs, the sensitivity of FGFR-3 detection can reach to 0.033 fM (S/N = 3) with a linear range from 0.1 fM to 1 nM. This biosensor has shown successful detection of the gene mutation in complex spiked samples.

Usually, hypertension therapies targeting the adrenoceptor beta-1 (ADRB1) gene and may cause gene mutation. A highly sensitive electrochemical biosensor was designed to detect ADRB1 gene mutation (Yuan et al., 2017). Otherwise, the above mentioned electrochemical biosensors consist of only one unit that is working as the capture and signal unit. GCE was modified with a nanocomposite of Fe-MIL-88-NH_2, hemin, Pt NPs, and Cu(II) ions (Fig. 7). Then H_2O_2 was added to the solution. The H_2O_2 reduction was catalyzed rapidly by Pt/hemin@Fe-MIL-88NH_2/Cu^{2+}. The addition and immobilization of the probe on the electrode have a slight effect on the electrocatalytic reduction activity of the composite. With the introduction of the target ssDNA and hybridization, the electrocatalytic activity sharply decrease. The target ADRB1 gene concentration is directly proportional to the decrease in the signals, and so can be detected up to 0.21 fM (S/N = 3). The prepared assay has displayed a successful detection of ADRB1 gene mutation in complex spiked serum samples.

To the best of our knowledge, all MOF based electrochemical DNA biosensors are reported in Table 2. As shown in this table, all methods are highly sensitive and selective to single base mismatched DNA and were tested on spiked serum samples. However, it has been tested neither on real clinical samples nor for cross-reactivity. Moreover, all methods are time-consuming (2–4 h). Regarding the LOD, method number 3 is the highest sensitive, but it takes the longest detection time 4 h. Based on the reported data the method number 4 is the most effective method because it has a good LOD and is based on using only one unit that working as the capture and signal unit.

3.3. Colorimetric technique

It can be used to design simple, rapid, and cost-effective DNA biosensor. A sensitive colorimetric biosensor was designed for HIV-ssDNA detection, based on a composite of Fe-MIL-88, and AuNPs (Liu et al., 2014). This composite catalyses the oxidation reaction of 3,3′,5,5′-tetramethylbenzidine (TMB) with H_2O_2, and the solution color becomes blue. On the addition of the probe-ssDNA to the solution, it is adsorbed on the surface of Au@Fe-MIL-88 through the π- π stacking interactions and this is accompanied by a sharp decrease in the catalytic activity of the composite, the blue color solution changed to green. In the presence of the target HIV-ssDNA, the target hybridizes with the probe and release it away from the composite surface and that is accompanied by the recovery of the catalytic activity of the composite, the green color of the solution changed to blue. The target HIV-ssDNA can't be detected lower than 11.4 nM, which isn't a good detection limit compared to other methods.

4. RNA sensing based on MOFs

Ebolaviruses, including Ebola virus and Sudan virus (SUDV), are non-segmented negative-sense RNA viruses that cause hemorrhagic fevers in humans and animals (Basler, 2015). Thus, early diagnosis of

Table 4
MOFs based fluorescent biosensors for miRNA detection.

Meth. No.	Target/Year	Metal Precursor/Ligand/Solvent/Modulator	Synthesis	Structure	Q_E%	DT	DR(nM)	LOD (pM)	Cross Reactivity	Clinical Samples	Ref.
1	miR-21, miR-96, miR-125b/2015	$ZrCl_4$/TPA/DMF	Solvothermal	3D	81.6	1.5–3 h	0–1000	10	tested	–	Wu et al. (2015)
2	miR-185/2017	$Cu(NO_3)_2$/H_3dcbBr/H2O	Hydrothermal	1D	87 ± 5	13 ± 3 m	0–80	172 ± 5	tested	–	Qiu et al. (2017)
	miR-20a/2017	$Cu(NO_3)_2$/H_2dcbBr/H2O	Hydrothermal	1D	94 ± 3	14 ± 2 m	0–100	321 ± 8	tested	–	Qiu et al. (2017)
	miR-92b/2017	$Cu(NO_3)_2$/H_3dcbBr/H2O	Hydrothermal	1D	77 ± 8	15 ± 2 m	0–100	91 ± 7	tested	–	Qiu et al. (2017)
	miR-25/2017	$Cu(NO_3)_2$/H_2dcbBr/H2O	Hydrothermal	1D	95 ± 2	19 ± 1 m	0–70	559 ± 8	tested	–	Qiu et al. (2017)
	miR-210/2017	$Cu(NO_3)_2$/H_2dcbBr/H2O	Hydrothermal	1D	96 ± 4	38 ± 3 m	0–80	132 ± 12	tested	–	Qiu et al. (2017)
3	miR-21/2017	$MnCl_2$/DMS/H2O	Hydrothermal	2D	N.D	4–8 h	0.0005–0.1	N.D	–	–	Song (2017)

*All methods have high specificity to single base mismatched miRNA.

these viruses is highly needed for infection/s control and management. Now, the development of a sensitive, specific, and cost-effective RNA detection method is critical for the diagnosis of viruses' diseases. In this section, RNA sensing based on MOFs using fluorescence technique will be discussed, as the only technique used.

A highly sensitive and cost-effective RNA biosensor was designed to detect Sudan virus RNA sequences based on a water-stable three-dimensional (3D) Cu-MOF (Yang et al., 2015a,b,c). The ssDNA probe was immobilized on the MOF surface via π-π stacking, hydrogen bonding, and electrostatic interactions, and so the fluorescence is quenched (Fig. 8). The addition of the target RNA results in hybridization with the probe and that is accompanied by release of the FAM dye from the MOF surface and recovery of the fluorescence. This assay provided a high LOD up to 73 pM. The prepared biosensor was tested for cross-reactivity with HIV-DNA, and there wasn't any cross-reactivity.

A similar strategy was pursued for designing another SUDV RNA biosensor (Yang et al., 2017). La-MOFs provides good luminescence due to f-f transitions (Zhao et al., 2015a,b). Two water-stable La-MOFs were synthesized; first with 3D structure and the second with 2D structure. Both can absorb the FAM-tagged probe DNA (P-DNA) and quench the FAM fluorescence via photoinduced electron transfer (PET) (Atchison et al., 2015; Daly et al., 2015; Zhang et al., 2010). The addition of the target SUDV RNA to the P-DNA@1 or P-DNA@2 system results in a stable DNA@RNA duplex. The formation of the duplex takes the P-DNA away from the surfaces of MOFs 1 and 2, accompanied by the fluorescence recovery. The target, SUDV RNA, can be detected over the range from 0 to 50 nM with a LOD of 112 pM with a RSD of 1.2% and 67 pM with a RSD of 1.1%, respectively. The reported results refer to MOF with 2D structure is more effective than 3D, in RNA detection. This performance can be explained due to the surface area exposed to probe immobilization and so target hybridization, in 2D is higher than 3D.

Infection caused by Ebola virus is an acute, and so the early diagnosis of Ebola virus nucleic acid is urgent for infection control. RNA biosensor was developed for detection of Ebola virus RNA, which is based on 3D dysprosium MOF (Qin et al., 2016) that has the ability to quench the labeled FAM probe through electrostatic, π-stacking and/or hydrogen bonding interactions and hence the fluorescence intensity recovered by about 65% after the addition of Ebola virus RNA sequences, and this method reported a high LOD up to 160 pM.

Dengue virus (DENV) and Zika virus (ZIKV) are two of the acute diseases that are seriously affecting many countries (Boeuf et al., 2016), and pose large threat to human's health for their high morbidity and mortality rate, so early diagnosis is essential especially in the infections outbreaks for controlling the infection.

RNA biosensor was developed for Dengue and Zika virus RNA detection, based on Cu-MOF (Xie et al., 2018). It also has the ability to quench the fluorescent labeled specific probe/s and upon the addition of the target, the fluorescence restored. This assay displayed a sensitive DENV and ZIKV detection up to 332 and 192 pM with the single detection method, while 184 and 121 pM can be reached with the synchronous fluorescence detection method, respectively. There was no cross-interaction between the two probes for synchronous detection. The good performance of synchronous fluorescence technique is attributed to the Raleigh light scattering wasn't interfere with the fluorescence signal.

Table 3 shows the four methods that have high specificity to single base mismatched RNA, in addition to methods number 1 and 4 were tested for cross-reactivity while others not. However, all methods weren't tested on real human samples or even on spiked serum samples. There isn't an optimum method, but regarding the detection time, method number 4 is the best; however, it has a moderate sensitivity. Accordingly, we considered method number 2 is the most effective one as it provides a good detection time with the highest sensitivity, 67 pM.

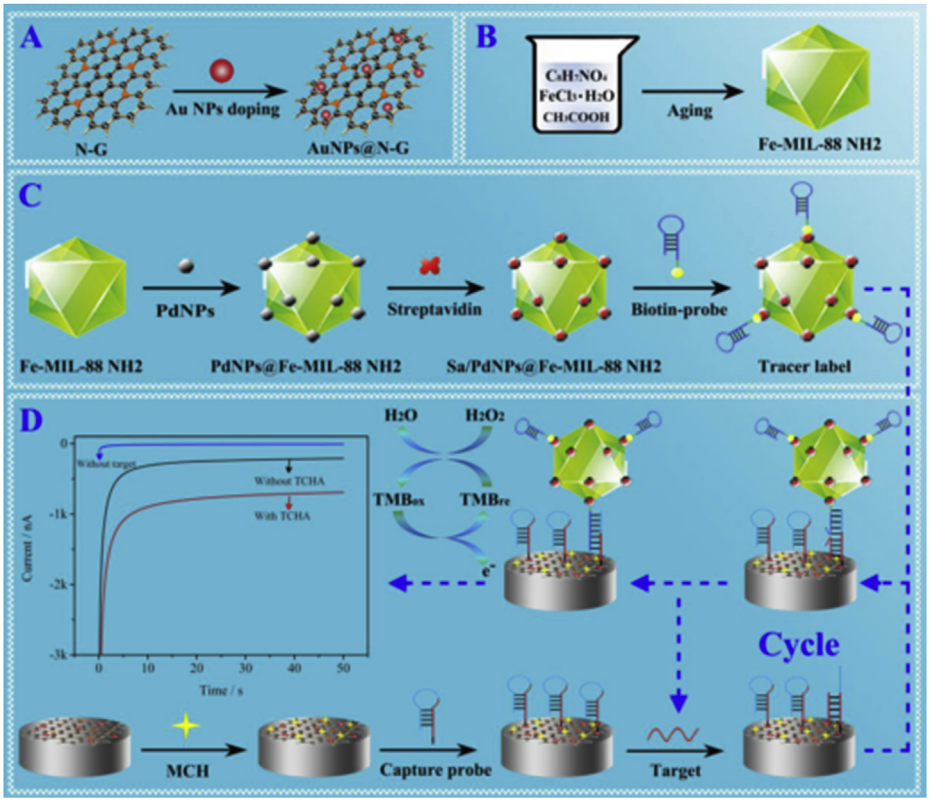

Fig. 10. Illustration of the electrochemical biosensor. (A) The preparation process of AuNPs@N-G (B) Fe-MIL-88NH_2 MOFs, (C) PdNPs@Fe-MOFs/SA/SPs bioconjugates (D) The fabrication process of the biosensor and the target-catalyzed hairpin assembly for target recycle. (Reprinted with permission from ref. (Li et al., 2017). Copyright 2017, Elsevier).

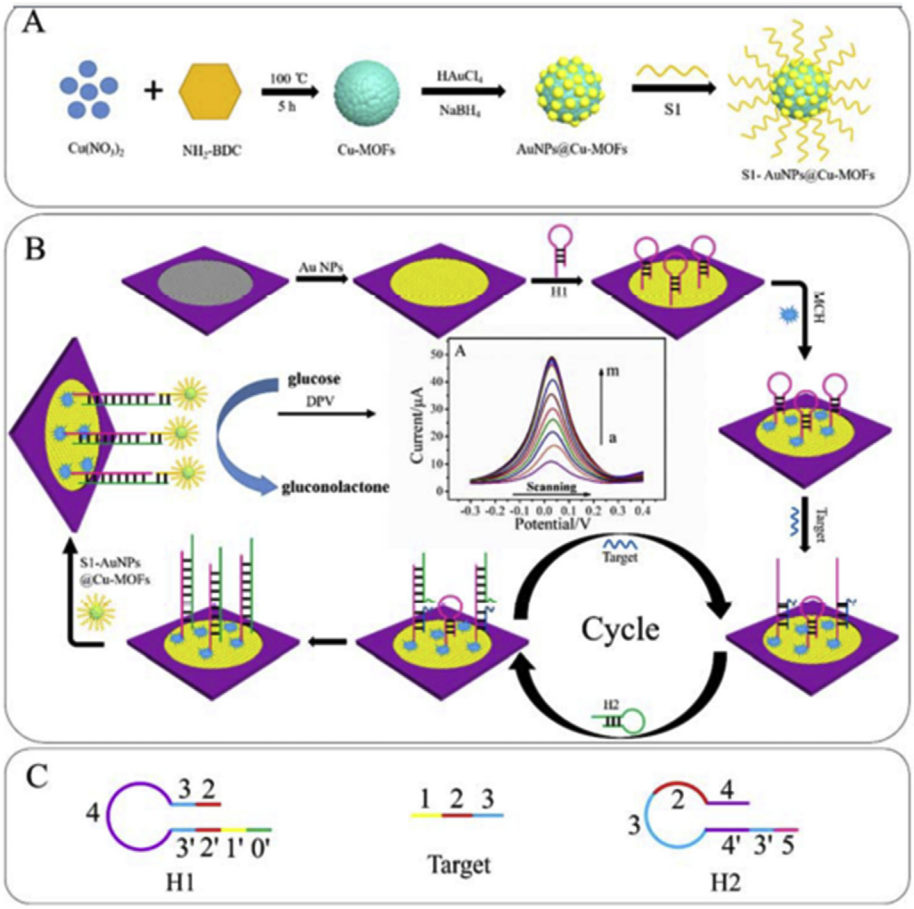

Fig. 11. Schematic illustration of the fabrication of the biosensor: (A) Preparation procedure of S1-AuNPs@Cu-MOFs; (B) The detection principle for glucose and the strategy of signal amplification. (C) Structure of H1, target, and H2. (Reprinted with permission from ref. (Wang et al., 2017). Copyright 2017, Elsevier).

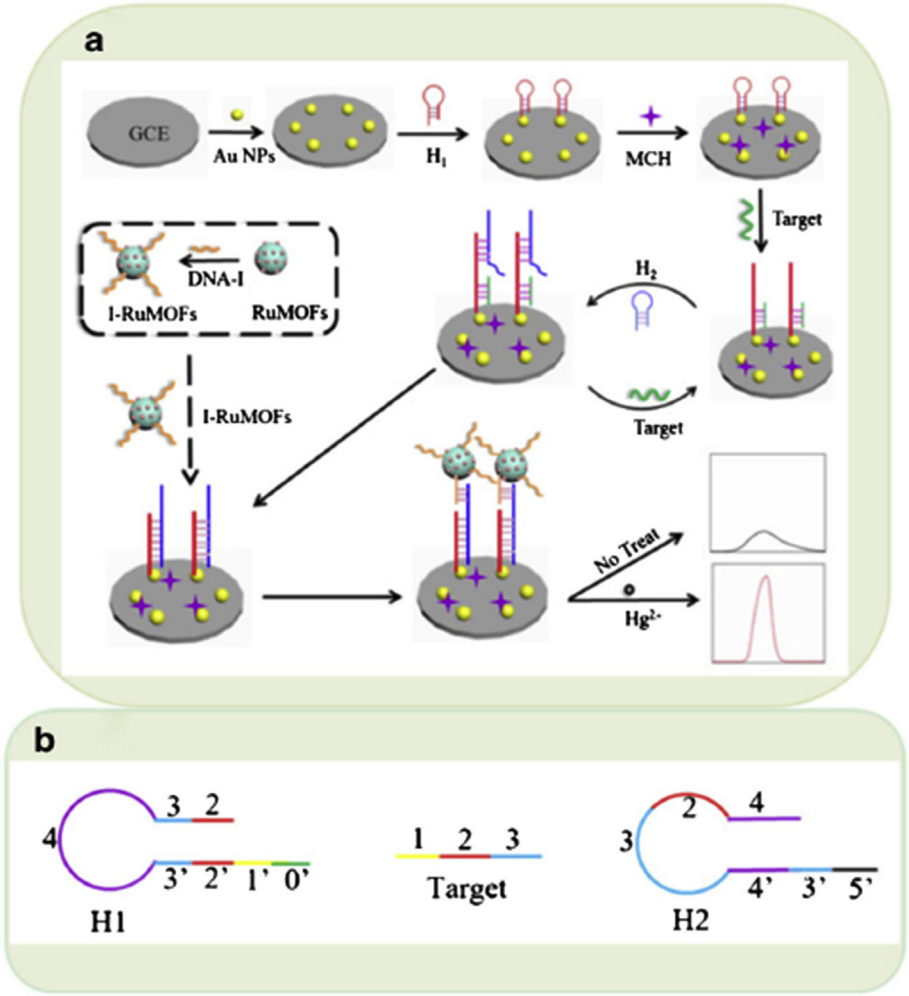

Fig. 12. (a) Schematic representation for detection of miRNA-155 and the strategy of signal amplification (GCE: glassy carbon electrode; Au NPs: Au nanoparticles; H1: capture hairpin probe; MCH: 6-mercapto-1- hexanol; H2: hairpin DNA; I- RuMOFs: tris(bipyridine)ruthenium(II) functionalized metal organic framework materials modified by DNA strand-I); (b) Structure of H1, target and H2 (base pairing com- plementary parts: 1–1′,2–2′,3–3′, 4–4′). (Reprinted with permission from ref. (Jian et al., 2018). Copyright 2018, Springer).

5. miRNA sensing based on MOFs

MicroRNA (miRNA) is a small sized RNA that is an important biomarker since the abnormal expression of specific miRNA is associated with many diseases including cancer (Liao and Ju, 2015). Thus, the development of ultra-sensitive biosensors for miRNA detection is urgent for early diagnosis of many diseases. miRNA biosensors are mainly constructed based on FL, EC and/or ECL techniques, so, MOFs based miRNA sensing regarding these techniques will be discussed.

5.1. Fluorescence technique

A highly sensitive and selective biosensor was designed for multiplexing monitoring of miR-21, miR-96 and miR-125b, in cancer cells (Wu et al., 2015). Accordingly, FAM-PNA21, Cy5-PNA96, and ROX-PNA125b were chosen as probes. UiO-66 worked as a fluorescence quencher of the labeled PNA that is firmly bound with the metal center. The metal ions Zr^{4+} in UiO-66 played a key role in fluorescence quenching via PET effect (Wei et al., 2013). The addition of the target is accompanied by PNA hybridization and so released from the MOF surface and then fluorescence recovery as shown in Fig. 9. And so, the target can be sensed up to 10 pM.

Qiu et al., 2017 reported a miRNA biosensor that designed to recognize five gastric cancer-associated miRNAs, 185, 20a, 92b, 25 and miR-210 (Qiu et al., 2017). Therefore, five labeled probes ssDNA are used (P-DNA). Cu-MOF was used as a fluorescence quencher through interaction with the P-DNA. The introduction of the complementary target miRNA to the corresponding P-DNA@MOF system would lead to the formation of stable and rigid P-DNA@RNA hybrid duplex. The formed hybrid duplex releases the P-DNA away from the surface of MOF, thereby stop up the PET process and leading to the fluorescence recovery. This method is successful in detection of multiplexed miRNAs, with LOD ranging from 91 to 559 pM.

Another miRNA biosensor was developed for detection of miR-21, which was expressed in cancer cell lines, Michigan cancer foundation-7 (MCF-7 cells) (Song, 2017). This method based on ultrathin Mn-MOF nanosheets as sensing platforms and HCR technique to increase the sensitivity. This method is very effective and the miRNA can be sensed over the linear range of 0.5–100 pM.

Table 4 represents all methods that have high specificity up to single base mismatched miRNA, however, all methods haven't been tested for real human samples or even for spiked serum samples. Despite method number 1, is the most sensitive one, it is not rapid, and the detection takes up to 3 h. In the same context, method 2 is rapid however it has a moderate sensitivity. Moreover, method number 3, is time-consuming, up to 8 h, and its detection limit wasn't detected. Thus, there isn't an optimum assay.

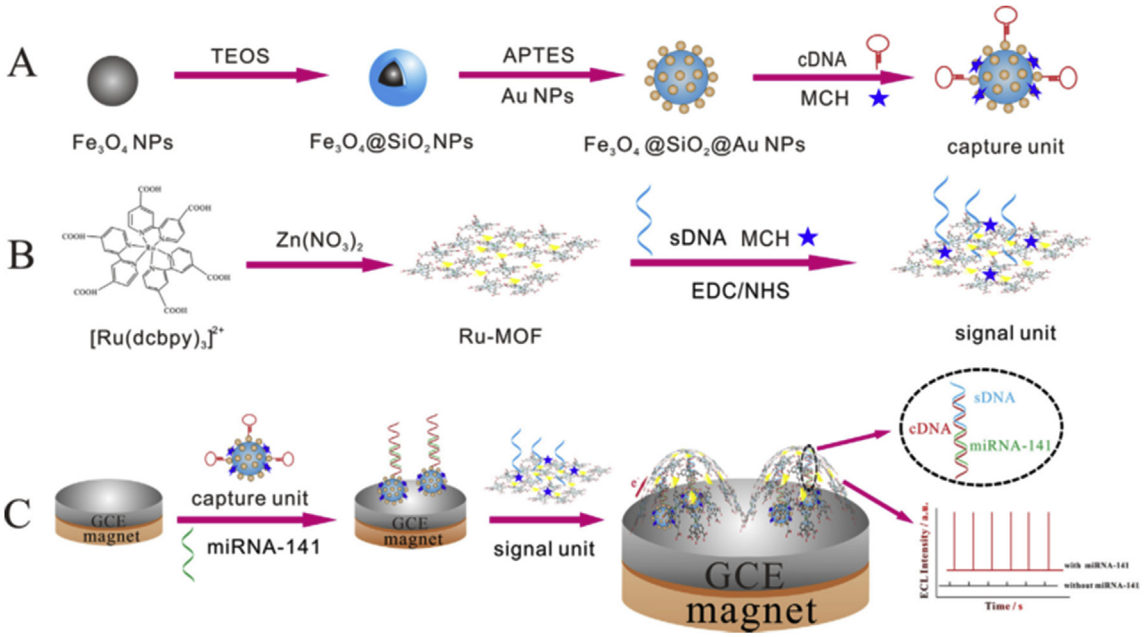

Fig. 13. Schematic diagram for **(A)** The preparation of capture unit Fe_3O_4@SiO_2@Au-cDNA, **(B)** The preparation of signal unit Ru-MOF-sDNA, and **(C)** The fabrication of the Faraday-cage ECL biosensor for miRNA-141 detection. (Reprinted with permission from ref. (Shao et al., 2018). Copyright 2018, Elsevier).

5.2. Electrochemistry and electrochemiluminescence techniques

miRNAs sensitive detection is a critical demand, which is conductive to acquaintance the biological processes accompanied by the disease (Yang et al., 2015a,b,c; Zhu et al., 2014). There are several methods for miRNA detection such as fluorescence (Yang et al., 2016), electrochemistry (Wang et al., 2016), colorimetry (L. Li et al., 2016), microanalysis (Donnem et al., 2011; Nelson et al., 2004) and other methods (Wang et al., 2019). One of the best detection methods is the electrochemical method because of the advantages of short response time, remarkable sensitivity, and cost-effective (Chen et al., 2017a,b; Hou et al., 2015; R. Li et al., 2016; Ren et al., 2013; Wang et al., 2014a,b).

An electrochemical biosensor was developed to detect miRNA-122, a biomarker of drug-induced liver injury (Li et al., 2017). In this biosensor, the signal unit (tracer label) is a nanocomposite of Fe-MIL-88-NH_2, palladium nanoparticles (PdNPs), Streptavidin, and hairpin signal probe (H2). This nanocomposite has excellent catalytic properties that simulate the peroxidase effect on the reaction of TMB oxidation in the presence of hydrogen peroxide. On the other side, the capture unit is represented by the GCE modified with AuNPs@N-G (nitrogen-doped graphene sheets) and hairpin capture probe (H1). On target miR-122 addition, the capture probe H1 will be opened and hybridized with the target. And then the signal unit addition leads to the releasing of the target from the H1-target hybrid and forms H1–H2 hybrid, and then the signal unit addition leads to the releasing of the target from the H1-target hybrid and forms H1–H2 hybrid, which has higher stability (Fig. 10). The released target started new hairpin-target recycling processes that result in a large number of signal probes attached to the electrode surface and a significant positive effect on the signal amplification. According to this assay, the target miR-122 can be sensed up to 0.003 fM with a linear range from 0.01 fM to 10 pM. This assay was successfully applied on complex spiked serum samples in addition to providing excellent recovery and selectivity on real human serum samples for the first time.

A similar strategy was pursued by the detection of miRNA-155 detection (Wang et al., 2017). But, the signal unit was a composite, with catalytic oxidation properties, of Cu-MOF, AuNPs and signal probe, S1-AuNPs@Cu-MOFs. And the capturing unit was a paper-based electrode treated with AuNP layer and hairpin DNA fragment probe H1. And then MCH was added to block any nonspecific active sites on the electrode. The addition of miRNA-155 is accompanied by opening the hairpin probe H1 and hybridization with the opened probe. And then the addition of another probe (H2) leads to, displacement of the target from the H1-target hybrid and forming H1–H2 hybrid with higher stability (Fig. 11). The released target will enter new hairpin-target recycling processes. In the formed H1–H2 hybrid, H2 is longer than H1, so, the remainder H2 fragment is ready for hybridization with signal probe (S1) on the addition of the signal unit, S1-AuNPs@Cu-MOFs. In the presence of glucose, the catalytic glucose oxidation effect of AuNPs@Cu-MOFs has a remarkable effect on the electrical signal readout. So, the LOD was significantly improved to reach 0.35 fM with a linear range from 1.0 fM to 10 nM. This assay allows successful miRNA-155 detection in complex spiked serum samples.

As indicated, the electrochemistry technique has a lot of advantages that when mixed with the merits of the chemiluminescence technique, lead to the ECL technique. The principle of working of ECL biosensor is like that of EC biosensors. As mentioned before, MOF composites are only used in electrochemical NAs biosensors due to the poor electrical conductivity of pure MOFs, except Ruthenium MOF (Ru-MOF) that has excellent conductivity and an intrinsic electrochemical luminescence so it can be used in ECL biosensors. miRNA-155 has been detected by Mercury-triggered ECL biosensor (Jian et al., 2018). The signal probe (I) attached to the Ru-MOF, represent the signal unit. While the capture unit is represented by GCE modified with AuNPs and a hairpin capture probe (H1) and then treated with MCH to block any unspecific active sites. The miRNA-155 addition results in the formation of H1-target hybrid through hybridization. After the addition of the probe H2, the target was displaced and released from its hybrid with H1, and a new hybrid H1– H2 was formed with higher stability Fig. 12. The target became free and entered in a new hybridization cycle. On the addition of the signal unit, I-RuMOF, the remaining single fragments of H2 can combine with the signal probe, I. Finally, mercury (Hg^{2+}) was added to the solution and consequently, the solution color changed from a feebly red color to bright red. This is attributed to the intrinsic property of Ru-MOFs, Hg^{2+} triggered the release of $Ru(bpy)_3^{2+}$ from Ru-MOFs. Consequently, the electrical signals largely magnified. This method has displayed a high sensitivity to miRNA-155 detection up to 0.3 fM. This

Table 5
MOFs based miRNA biosensors according to electrochemistry and electrochemiluminescence methods.

Meth. No.	Target/Year	Metal Precursor/Ligand/Solvent/Modulator	Composite	Synthesis	DM	Electrode	DM	DT (h)	DR	LOD (fM)	Cross Reactivity	Clinical Samples	Ref.
1	miR-122/2017	$FeCl_3$/2ATPA/PEI/DMF/AcOH	PdNPs@ Fe-MOFs	Solvothermal	EC	GCE/AuNPs@ N-G	CV, EIS, DPV	1.25	0.01 fM- 10 pM	0.003	–	Sp. serum & Blood	Li et al. (2017)
2	miRNA-155 /2017	$Cu(NO_3)_2$/2ATPA/DMF:EtOH/PVP	AuNPs@ Cu-MOFs	Solvothermal	EC	PWE/AuNPs	CV,EIS, DPV	4	1 fM-10 nM	0.35	–	Sp. serum	Wang et al. (2017)
3	miRNA-155 /2018	$Zn(NO_3)_2$/BPDC, adenine, $Ru(bpy)_3Cl_2$/DMF:H_2O/ HNO_3	–	Solvothermal	ECL	GC/AuNPs	CV,EIS	4	0.8 fM-1 nM	0.3	–	Sp. serum	Jian et al. (2018)
4	miRNA-141 /2018	$Zn(NO_3)_2$/$[Ru(dcbpy)_3]^{2+}$/PrOH:H_2O	–	Sonication	ECL	MGCE/Fe_3O_4 @SiO_2@Au	CV,EIS	2	1 fM- 10 pM	0.3	–	Sp. serum	Shao et al. (2018)

***immobilization in all methods in the table via Au-S bond and all methods have high specificity to single base mismatched miRNA; DM**: detection method; **HKUST**: Hong Kong University of Science and Technology; **H_3BTC**: 1,3,5-benzene-tricarboxylic acid; **N-G**: nitrogen dopped grapheme; **PEI**: polyethyleneimine; **$Ru(bpy)_3Cl_2$**: tris(bipyridine) ruthenium (II); **BPDC**: 4,4′-biphenyldicarboxylate; **$[Ru(dcbpy)_3]^{2+}$**: tris (4,4′-dicarboxylicacid-2,2′-bipyridyl) ruthenium(II); **PrOH**: n-propanol; **MGCE**: magnet glassy carbon electrode; **PWE**: paper working electrode; **EC**: electrochemistry; **ECL**: electrochemiluminescence.

assay allows successful miRNA-155 detection in spiked complex serum samples.

Also, ECL biosensor was developed for miRNA-141 detection, based on Faraday-cage (Shao et al., 2018). The signal unit can be represented by a signal probe (sDNA) immobilized on Ru-MOF. And the capture unit was nano-composite of Fe_3O_4@SiO_2@Au labeled by capture hairpin probe “capture deoxyribonucleic acid (cDNA)” and coated on a magnetic glassy carbon electrode (MGCE). miRNA-141 addition is accompanied by opening the hairpin cDNA probe and hybridization with the opened probe. The remainder unhybridized fragment of the capture probe is ready for further hybridization with the complementary signal probe, once the signal unit added. Therefore, the Faraday-cage structure was formed and so all the molecules of the signal unit are electroactive and subsequently, the ECL signals were magnified Fig. 13. Consequently, the sensitivity of miRNA-141 detection increased to 0.3 fM over a linear range from 1 fM to 10 pM. The selectivity and reproducibility of this biosensor were validated and it is successfully applied to spiked complex serum samples with recoveries up to 110%.

Table 5 represents all EC and ECL methods have high sensitivity and specificity to single base mismatched, and successfully tested for spiked serum samples, however, all methods haven't been applied on real clinical samples, except the first method. Also, all methods weren't tested for cross-reactivity and take a long detection time ranging from 1.2 to 4 h. By comparing the two EC methods with each other, the first method is better regarding lower detection time, sensitivity, and applicability on real human samples. On the other side, by comparing the two ECL methods with each other, method number 4 is better regarding lower detection time. Finally, by comparing all methods in Table 5, method number 1 is the best regarding the detection time, the ultrasensitivity and the only one applied to real samples.

6. Conclusions and future perspectives

In summary, based on the findings in this review, MOFs are considered to be a rapidly evolving tool that can be effectively used for NAs biosensing. MOFs as NAs biosensors development have been extensively outlined in this review from a broad perspective, such as synthesis, manipulation, different sensing methods (fluorescence, electro, etc.), which makes them as potential NAs biosensors that meet the rigorous demands in clinical laboratories, as high sensitivity and specificity. However, many challenges should be overcome to achieve potential, reproducible, and feasible MOFs based biosensors. These challenges could be simply expressed as (i) design, synthesis, and stability of the MOFs, and (ii) applying on real clinical samples.

The first challenge, for example, could be expressed briefly as: crystallization process of MOF should be controlled to adjust the particle size of MOFs, the coexistence of micro-pores and macro-pores in MOFs structure should be monitored and controlled during design & synthesis, as the MOF structure is the prime stone for developing the biosensor efficiency. Moreover, MOFs stability is the urgent factor for the reusability and regeneration after the addition of target, so it is required to improve the stability of MOFs. In addition, the large incubation time required to get the EC and ECL signals that reach in some biosensors up to 4 h, which may be attributed to the poor conductivity of MOFs. This could be improved by using composites with good conductive materials such as conducting polymers, and also some new methodologies, such as calcination or pyrolysis, are being applied to improve the conductivity of the MOFs. These improvements will add an important step of the MOFs in the POC testing.

On the other side, the second challenge or drawback of the MOFs is almost all the designed and tested MOFs based NA sensing system haven't been tested on real clinical samples, which is completely different from testing synthetic target/s.

Future fluorescent biosensors should focus on F-group elements, especially lanthanides, due to its intrinsic visible, pure color, and also have excellent luminescence on account of f-f transition. Based on

structure comparison done along with this review, it was shown that 2D MOFs are the best structure as a quencher for NAs sensing, due to the high surface area they provided. Thus, enhancing of 2D MOFs properties may lead to better sensitivity and specificity, bearing in mind more studies on the 1D and 2D structures. On the other side, functionalization of MOFs with different groups having several properties could obviously enhance the general performance. Also, MOFs composites with other materials should be widely tested as a quencher to improve the sensitivity, specificity, detection time, and cost-effectiveness. Moreover, MOF composites, in EC and ECL NAs biosensors may be an option for improving the electrical conductivity of the MOFs and hence, avoiding the drawbacks associated with the EC & ECL MOFs based biosensor. Furthermore, electrical biosensors should focus on using only one MOF unit that working as capturing and signal unit, as it is very cost effective.

In conclusion, MOFs as a sensing platform for NAs detection have made great progress in studies, but a lot of work is needed in the direction of designing an optimum biosensor with ultra-sensitivity, high specificity, simultaneous detection, simplicity in design and cost-effective. This highly dynamic research field is expected to influence the biosensors field positively and could be used in clinical diagnostics within the next few years.

Conflicts of interest

The authors declare no conflicts of interest.

Declaration of interests

The authors declare that they have no known competing financial interests or personal relationships that could have appeared to influence the work reported in this paper.

CRediT authorship contribution statement

Diaa I. Osman: Writing - original draft. **Said M. El-Sheikh:** Writing - original draft, Formal analysis. **Sheta M. Sheta:** Formal analysis, Writing - original draft. **Omnia I. Ali:** Writing - original draft. **Aliaa M. Salem:** Writing - original draft. **Wafaa Gh Shousha:** Writing - original draft. **Sherif F. EL-Khamisy:** Writing - original draft. **Sherif M. Shawky:** Formal analysis, Writing - original draft.

Acknowledgments

We thank Prof. Dr. Khalid Hassan and Dr. Ahmed Zohair for providing insight and expertise that greatly assisted to achieve this work. This work was financially supported by the Zewail City of Science and Technology, Egypt, by a Zewail City Program Grant to S.F.E-K.

References

An, J., Shade, C.M., Chengelis-czegan, D.A., Rosi, N.L., 2011. J. Am. Chem. Soc. 5, 1220–1223.
Asha, K., Kumar, P., Khanna, M., Kumar, B., 2019. J. Clin. Med. 8, 1–24.
Atchison, J., Kamila, S., Callan, B., Mchale, P., Callan, J.F., 2015. Chem. Commun. 51, 16832–16835.
Basler, C.F., 2015. Virology 13, 122–130.
Boeuf, P., Drummer, H.E., Richards, J.S., Scoullar, M.J.L., Beeson, J.G., 2016. BMC Med. 14, 1–9.
Butova, V.V., Soldatov, M.A., Guda, A.A., Lomachenko, K.A., Lamberti, C., 2016. Russ. Chem. Rev. 85, 280–307.
Carrasco, S., 2018. Biosensors 8, 1–30.
Carson, C.G., Brown, A.J., Sholl, D.S., Nair, S., 2011. Cryst. Growth Des. 10, 4505–4510.
Chen, L., Zheng, H., Qiu, B., Chen, G., Chen, Z.N., 2013. Analyst 138, 3490–3493.
Chen, Y.X., Huang, K.J., Lin, F., Fang, L.X., 2017a. Talanta 175, 168–176.
Chen, Y.X., Huang, K.J., Niu, K.X., 2017b. Biosens. Bioelectron. 99, 612–624.
Chen, Y.X., Wu, X., Huang, K.J., 2018. Sensor. Actuator. B Chem. 270, 179–186.
Cheong, V.F., Moh, P.Y., 2018. Mater. Sci. Technol. 34, 1025–1045.
Chidambaram, A., Stylianou, K.C., 2018. Inorg. Chem. Front. 5, 979–998.
Crane, J.L., Anderson, K.E., Conway, S.G., 2015. J. Chem. Educ. 92, 373–377.
Daly, B., Ling, J., Silva, A.P. De, 2015. Chem. Soc. Rev. 44, 4203–4211.
Dey, C., Kundu, T., 2014a. Cryst. Eng. 70, 1–8.
Dey, C., Kundu, T., 2014b. Acta Crystallogr. B 23, 3–10.
Dharmarathna, S., King, C.K., Pedrick, W., Pahalagedara, L., Suib, S.L., 2012. Chem. Mater. 24, 705–712.
Donnem, T., Eklo, K., Bremnes, R.M., Busund, L., 2011. J. Transl. Med. 9, 1–9.
Driscoll, L.O., 2007. Anticancer Res. 27, 1257–1265.
Dybtsev, D.N., Chun, H., Kim, K., 2004. Angew. Chem. Int. Ed. 43, 5033–5036.
Fan, C., Plaxco, K.W., Heeger, A.J., 2003. Proc. Natl. Acad. Sci. Unit. States Am. 100, 9134–9137.
Fang, J.M., Leng, F., Zhao, X.J., Hu, X.L., Li, Y.F., 2014. Analyst 139, 801–806.
Farjami, E., Clima, L., Gothelf, K., Ferapontova, E.E., 2011. Anal. Chem. 83, 1594–1602.
Ferey, G., 2008. Chem. Soc. Rev. 37, 191–214.
Garay, A.L., Pichon, A., James, S.L., James, S.L., 2007. Chem. Soc. Rev. 36, 846–855.
Getachew, A., Cheneke, W., Shiferaw, B., Yaregal, A., Kebede, E., 2019. J. Trop. Med. 1, 1–8.
Guo, J.F., Li, C.M., Hu, X.L., Huang, C.Z., Li, Y.F., 2014. RSC Adv. 4, 9379–9382.
Halper, S.R., Do, L., Stork, J.R., Cohen, S.M., 2006. J. Am. Chem. Soc. 128, 15255–15268.
Haupt, K., Mosbach, K., 2000. Chem. Rev. 100, 2495–2504.
He, C., Lu, K., Liu, D., Lin, W., 2014. J. Am. Chem. Soc. 136, 5181–5184.
Hindelang, K., Vagin, S.I., Anger, C., Rieger, B., 2012. Chem. Comm. 2, 2888–2890.
Horcajada, P., Gref, R., Couvreur, P., Serre, C., 2012. Chem. Rev. 112, 1232–1268.
Hou, T., Li, W., Liu, X., Li, F., 2015. Anal. Chem. 87, 11368–11374.
Hou, L., Zhou, B., Li, Y., La, M., 2019. Int. J. Electrochem. Sci. 14, 4453–4468.
Howarth, A.J., Peters, A.W., Vermeulen, N.A., Wang, T.C., Hupp, J.T., Farha, O.K., 2017. Chem. Mater. 29, 26–39.
Huang, X., He, Z., Xiong, Y., Chen, X., 2018. Theranostics 8, 3461–3473.
Imaz, I., Cano-sarabia, M., Maspoch, D., Carne, A., 2013. Nat. Chem. 2, 1–9.
Jhung, S.H., Lee, J., Chang, J., 2005. Korean Chem. Soc. 26, 880–881.
Jia, J., Xu, F., Long, Z., Hou, X., Sepaniak, M.J., 2013. Chem. Commun. 49, 4670–4672.
Jian, Y., Wang, H., Liu, H., Ge, S., Yu, J., 2018. Microchim. Acta 2, 11–18.
Karina, A., Leite, P., Fagner, J., 2017. Res. 20, 681–687.
Kim, Y., Sohn, D., Tan, W., 2008. Int. J. Clin. Exp. Pathol. 1, 105–116.
Kim, J., Yang, S.T., Kim, J., Ahn, W.S., 2011. J. Mater. Chem. 21, 3070–3076.
Kirsch, J., Siltanen, C., Zhou, Q., Revzin, A., Simonian, A., 2015. Chem. Soc. Rev. 42, 733–8768.
Klinowski, J., Paz, A.A., 2011. Dalton Trans. 40, 321–330.
Korzeniowska, B., Nooney, R., Wencel, D., Mcdonagh, C., 2013. Nanotechnology 24, 1–20.
Lan, A., Li, K., Ki, W., Li, J., 2009. Angew. Chem. Int. Ed. 4, 2334–2338.
Lei, J., Qian, R., Ling, P., Cui, L., Ju, H., 2014. Trends Anal. Chem. 58, 71–78.
Li, L., Zhang, Y., Yan, M., Yu, J., 2016. Anal. Chem. 88, 5369–5377.
Li, R., Yin, B., Ye, B., 2016. Biosens. Bioelectron. 86, 1011–1016.
Li, Y., Yu, C., Yang, B., Liu, Z., 2017. Biosens. Bioelectron. 102, 307–315.
Liang, W., Alessandro, D.M.D., 2013. Chem. Commun. 49, 3706–3708.
Liang, W., Babarao, R., Alessandro, D.M.D., 2013. Inorg. Chem. 52, 12878–12880.
Liao, X., Ju, H., 2015. Chem. Comm. 51, 2141–2144.
Ling, P., Lei, J., Ju, H., 2015a. Biosens. Bioelectron. 71, 373–379.
Ling, P., Lei, J., Zhang, L., Ju, H., 2015b. Anal. Chem. 87, 3957–3963.
Liu, J., Lu, Y., 2007. J. Am. Chem. Soc. 129, 9838–9839.
Liu, S., Wang, L., Tian, J., Luo, Y., Chang, G., Asiri, A.M., 2012. Chempluschem 77, 23–26.
Liu, Y.L., Fu, W.L., Li, C.M., Huang, C.Z., Li, Y.F., 2014. Chim. Acta 861, 55–61.
Liu, X., Shuai, H.L., Liu, Y.J., Huang, K.J., 2016. Sensor. Actuator. B Chem. 235, 603–613.
Lucier, B.E.G., Chen, S., Huang, Y., 2018. Acc. Chem. Res. 51, 319–330.
Marrazza, G., Chianella, I., Mascini, M., 1999. Biosens. Bioelectron. 14, 43–51.
Martynenko, I.V., Litvin, A.P., Purcell-Milton, F., Baranov, A.V., Fedorov, A.V., Gun'ko, Y.K., 2017. J. Mater. Chem. B 5, 6701–6727.
Mckinstry, C., Cathcart, R.J., Cussen, E.J., Fletcher, A.J., Patwardhan, S.V., Sefcik, J., 2016. Chem. Eng. J. 285, 718–725.
Mehrotra, P., 2016. J. Oral Biol. Craniofacial Res. 6, 153–159.
Mejia-ariza, R., Rosselli, J., Corradini, R., Huskens, J., 2017. Chem. Eur J. 23, 4180–4186.
Mueller, U., Puetter, H., Hesse, M., Schubert, M., Wessel, H., Huff, J., Guzmann, M., 2011. U.S. Pat. No US 7968, 739 B2 1–30.
Nelson, P.T., Baldwin, D.A., Scearce, L.M., Oberholtzer, J.C., Tobias, J.W., Mourelatos, Z., 2004. Nat. Methods 1, 155–161.
Pachfule, P., Das, R., Poddar, P., Banerjee, R., 2011. Cryst. Growth Des. 1215–1222.
Pham, M., Vuong, G., Vu, A., Do, T., 2011. Langmuir 27, 15261–15267.
Pramanik, S., Zheng, C., Zhang, X., Emge, T.J., Li, J., 2011. J. Am. Chem. Soc. 12, 4153–4155.
Qin, L., Lin, L.X., Qiu, G.H., Chen, J.X., Chen, W.H., 2016. Chem. Commun. 52, 132–135.
Qiu, L., Li, Z., Wu, Y., Wang, W., Xu, T., Jiang, X., 2008. Chem. Commun. 23, 3642–3644.
Qiu, G.H., Lu, W.Z., Wang, T.R., Li, M.M., Chen, J.X., 2017. J. Inorg. Biochem. 177, 138–142.
Ren, Y., Deng, H., Shen, W., Gao, Z., 2013. Anal. Chem. 85, 4784–4789.
Rubio-martinez, M., Mardel, J.I., Lim, K., Hill, M.R., 2014. Sci. Rep. 4, 1–5.
Rubio-martinez, M., Hadley, T.D., Barton, T., Lim, K., Hill, M.R., 2016. ChemSusChem 9, 938–941.
Rubio-martinez, M., Imaz, I., Maspoch, D., Hill, M.R., 2017. Chem. Soc. Rev. 46, 3453–3480.
Seetharaj, R., Vandana, P.V., Arya, P., Mathew, S., 2019. Arab. J. Chem. 12, 295–315.
Seo, Y., Hundal, G., Tae, I., Kyu, Y., Jun, C., Chang, J., 2009. Microporous Mesoporous Mater. 119, 331–337.
Shao, H., Lu, J., Zhang, Q., Hu, Y., Wang, S., Guo, Z., 2018. Sensor. Actuator. B Chem. 268, 39–46.
Shawky, S., Bald, D., Azzazy, H., 2010. Clin. Biochem. 43, 1163–1168.
Sheta, S.M., El-sheikh, S.M., Abd-elzaher, M.M., 2018. Dalton Trans. 47, 4847–4855.

Sheta, S.M., El-sheikh, S.M., Abd-elzaher, M.M., 2019a. Anal. Bioanal. Chem. 411, 1339–1349.
Sheta, S.M., El-Sheikh, S.M., Abd-Elzaher, M.M., Wassel, A.R., 2019b. Appl. Organomet. Chem. 33, e4777.
Shuai, H.L., Huang, K.J., Chen, Y.X., Fang, L.X., Jia, M.P., 2016a. Biosens. Bioelectron. 89, 989–997.
Shuai, H.L., Huang, K.J., Xing, L.L., Chen, Y.X., 2016b. Biosens. Bioelectron. 86, 337–345.
Shuai, H.L., Wu, X., Huang, K.J., Zhai, Z.B., 2017. Biosens. Bioelectron. 94, 616–625.
Song, W., 2017. Talanta 170, 74–80.
Stock, N., Biswas, S., 2012. Chem. Rev. 112, 933–969.
Takashima, Y., Shimomura, S., Sugimoto5, Kunihisa, Kitagawa, S., 2011. Nat. Commun. 2, 1–8.
Tan, H., Tang, G., Wang, Z., Li, Q., Gao, J., Wu, S., 2016. Anal. Chim. Acta 940, 136–142.
Tian, J., Liu, Q., Shi, J., Sun, X., He, Y., 2015. Biosens. Bioelectron. 71, 1–6.
Tranchemontagne, D.J., Hunt, J.R., Yaghi, O.M., 2008. Tetrahedron 64, 8553–8557.
Turner, A.P.F., 2013. Chem. Soc. Rev. 42, 3184–3196.
Wang, J., 2000. Nucleic Acids Res. 28, 3011–3016.
Wang, G., Song, C., Kong, D., Ruan, W., Chang, Z., Li, Y., 2014a. J. Mater. Chem. 2, 2213–2220.
Wang, M., Fu, Z., Li, B., Zhou, Y., Yin, H., Ai, S., 2014b. Anal. Chem. 86, 5606–5610.
Wang, H., Wang, Y., Xu, Y., Huang, J., 2016. Biosens. Bioelectron. 80, 471–476.
Wang, H., Jian, Y., Ge, S., Yu, J., 2017. Sensor. Actuator. B Chem. 257, 561–569.
Wang, S., Mcguirk, C.M., Aquino, A., Mason, J.A., Mirkin, C.A., 2018. Adv. Mater. 30, 1–14.
Wang, Y.H., He, L.L., Huang, K.J., Chen, Y.X., Wang, S.Y., Liu, Z.H., Li, D., 2019. Analyst 144, 2849–2866.
Wei, X., Zheng, L., Qiu, B., Chen, G., 2013. J. Mater. Chem. B 1, 1812–1817.
Wu, Y., Han, J., Xue, P., Xu, R., Kang, Y., 2015. Nanoscale 7, 1753–1759.
Xi, Z., Wei, X., Zhenyu, L., Guo, L., 2013. Chem. Commun. 49, 1276–1278.
Xiao, Y., Qu, X., Plaxco, K.W., Heeger, A.J., 2007. J. Am. Chem. Soc. 129, 11896–11897.
Xie, Z., Ma, L., Kathryn, E., Jin, A., Lin, W., 2010. J. Am. Chem. Soc. 132, 922–923.
Xie, B.P., Qiu, G.H., Jiang, Z.H., Chen, J.X., 2018. Sensor. Actuator. B Chem. 254, 1133–1140.
Xu, Q., Kitagawa, H., 2018. Adv. Mater. 30, 1–3.
Yaghi, O.M., 1997. U.S. Pat. 5, 648 508 1–30.
Yang, C., Shi, K., Dou, B., Xiang, Y., Chai, Y., Yuan, R., 2015a. ACS Appl. Mater. Interfaces 7, 1188–1193.
Yang, N., Chen, X., Ren, T., Zhang, P., Yang, D., 2015b. Chem 207, 690–715.
Yang, S., Chen, S., Qiu, G., Chen, W.-H., 2015c. Anal. Chem. 87, 12206–12214.
Yang, L., Pan, W., Yu, Z., Li, N., Tang, B., 2016. Anal. Chem. 88, 1–8.
Yang, S., Zhao, W., Bai, L., Li, M., Chen, J.X., 2017. Inorg. Chem. 56, 14880–14887.
Ye, T., Liu, Y., Luo, M., Zhou, G., He, Z., 2014. Analyst 139, 1721–1725.
Yoo, Y., Varela-guerrero, V., Jeong, H., 2011. Langmuir 27, 2652–2657.
Yu, Y., Wu, J., He, J., 2016. Biosens. Bioelectron. 91, 892–899.
Yuan, G., Zhu, C., Liu, Y., Cui, Y., 2011. Chem. Comm. 47, 3180–3182.
Yuan, G., Wang, L., Mao, D., Wang, F., Zhang, J., 2017. Microchim Acta 184, 3121–3130.
Yuan, S., Feng, L., Yang, X., Li, J., Zhou, H.C., 2018. Adv. Mater. 30, 1–35.
Zhang, G., Zhao, N., Hu, X., Tian, J., 2010. Biomol. Spectrosc. 76, 410–417.
Zhang, H., Zhang, J., Huang, G., Du, Z., Jiang, H., 2014. Chem. Commun. 50, 12069–12072.
Zhang, Q., Wang, C.F., Lv, Y.K., 2018. Analyst 143, 4221–4229.
Zhao, J., Wang, Y., Dong, W., Wu, Y., Li, D., Zhang, Q., 2015a. Inorg. Chem. 3, 2–8.
Zhao, M., Wang, Y., Ma, Q., Huang, Y., Zhang, X., Ping, J., 2015b. Adv. Mater. 27, 7372–7378.
Zhao, H., Yang, S., Ding, N., Qin, L., Qiu, G., Hor, T.S.A., 2016a. Dalton Trans. 45, 5092–5100.
Zhao, H.Q., Qiu, G.H., Yang, S.P., Chen, W.H., Chen, J.X., 2016b. Anal. Chim. Acta 922, 55–63.
Zhao, S., Wu, L., Feng, J., Song, S., Zhang, H., 2016c. Inorg. Chem. Front. 3, 376–380.
Zheng, W., Hao, X., Zhao, L., Sun, W., 2017. Ind. Eng. Chem. Res. 42, 1–21.
Zhou, J., Tian, G., Zeng, L., Song, X., Bian, X., 2018. Adv. Healthc. Mater. 7, 1–21.
Zhu, G., Liang, L., Zhang, C., 2014. Anal. Chem. 86, 11410–11416.
Zou, X., Zhu, G., Hewitt, I.J., Sun, F., Qiu, S., 2009. Dalton Trans. 42, 3009–3013.